Academy of Sciences of Uzbekistan
Institute of Nuclear Physics

Joint Institute for Nuclear Research
Dubna, Russia
Avazbek NASIROV

Joint Institute for Nuclear Research

Contents of talk

1. Short information about synthesis of superheavy elements in heavy ion collisions.
2. Significance of nuclear reactions:
   a) Fission process in atomic power stations as a source electrical energy and heat;
   b) Application of different isotopes in nuclear medicine for diagnostic aims and cancer terapy;
3. Mass distribution of reaction products.
4. The role of shell structure of atomic nuclei in the nuclear reactions at low energy.
5. Non-equilibrium sharing of the excitation energy between reaction products

Introduction

Press Release 30.05.2012 21:27

Element 114 is Named Flerovium and E…Livermorium

IUPAC

International Union of Pure and Applied Chemistry

IU…ame **flerovium**, with sym… number **114** and the nam… for the element of ato…

Priority for the discovery of thes…llaboration between the Joint Institute for Nuclear Re… Lawrence Livermore National Laboratory (Livermore…

The name **flerovium** will honor t… Reactions where superheavy elements are synthes…990) – was a renowned physicist, author of the discovery …nium, pioneer in heavy-ion physics, and founder i… Research the Laboratory of Nuclear Reactions…

The name **livermorium** honors th… Laboratory. A group of researchers of this Laboratory with the heavy element research group of the Flerov Laboratory of Nuclear Reactions took part in the work carried out in Dubna on the synthesis of superheavy elements including element 116.

Mendeleev periodic table of the elements (2012)

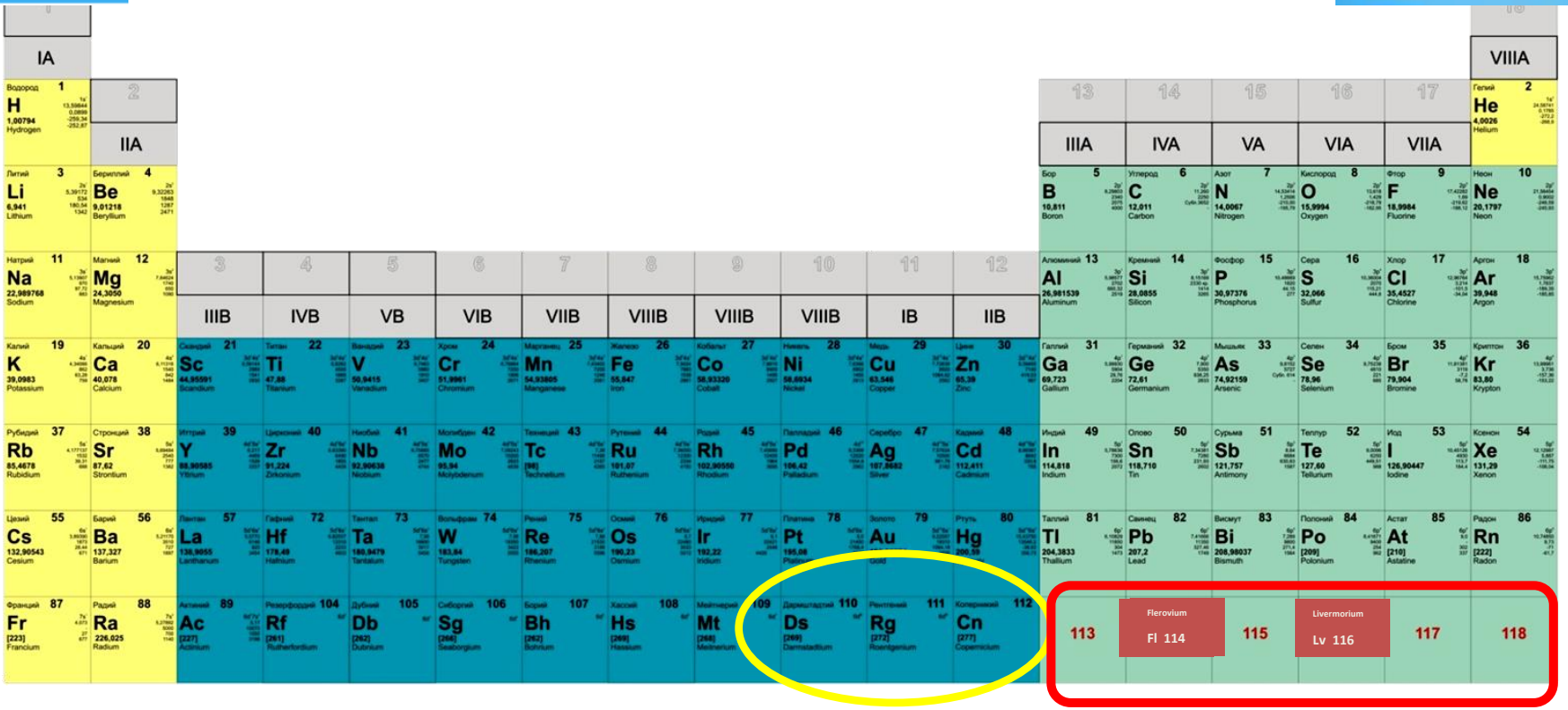

Лантаноиды Lanthanides

Актиноиды Actinides

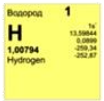

H - символ
1,00794 -атомный номер
1s¹ -электронная конфигурация
13,59844 -1-й потенциал ионизации, эВ
0,0899 - плотность кг/м³
-259,34 - температура плавления,°С
-252,87- температура кипения,°С

s-элементы
p-элементы
d-элементы
f-элементы

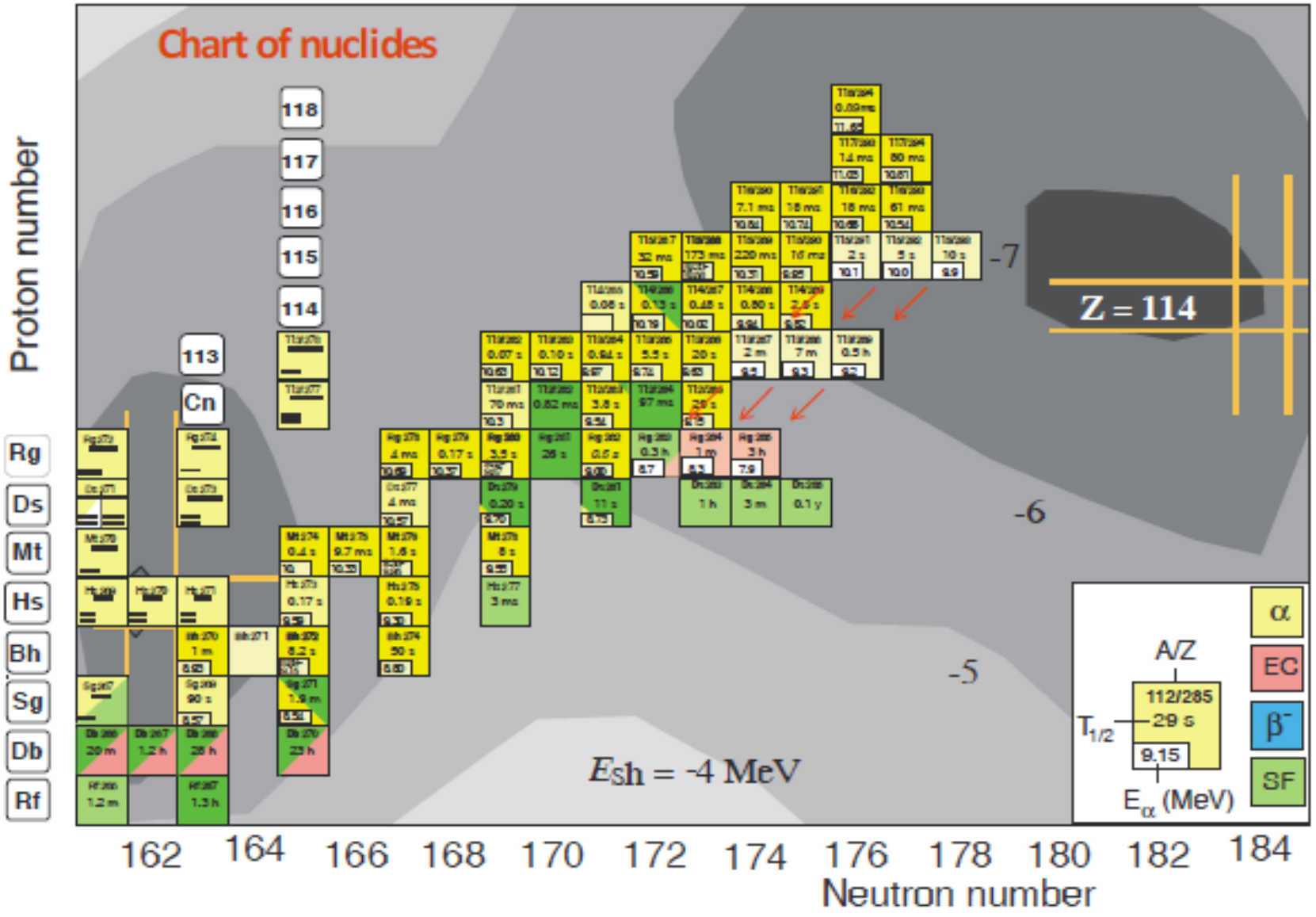
Chart of nuclides
Proton number
Neutron number
118
117
116
115
114
113
Cn
Rg
Ds
Mt
Hs
Bh
Sg
Db
Rf
162
164
166
168
170
172
174
176
178
180
182
184
-7
-6
-5
Z = 114
E_{sh} = -4 MeV
A/Z
112/285
$T_{1/2}$
29 s
9.15
E_α (MeV)
α
EC
β⁻
SF

Searching for the island of stability (GSI, Darmstadt)

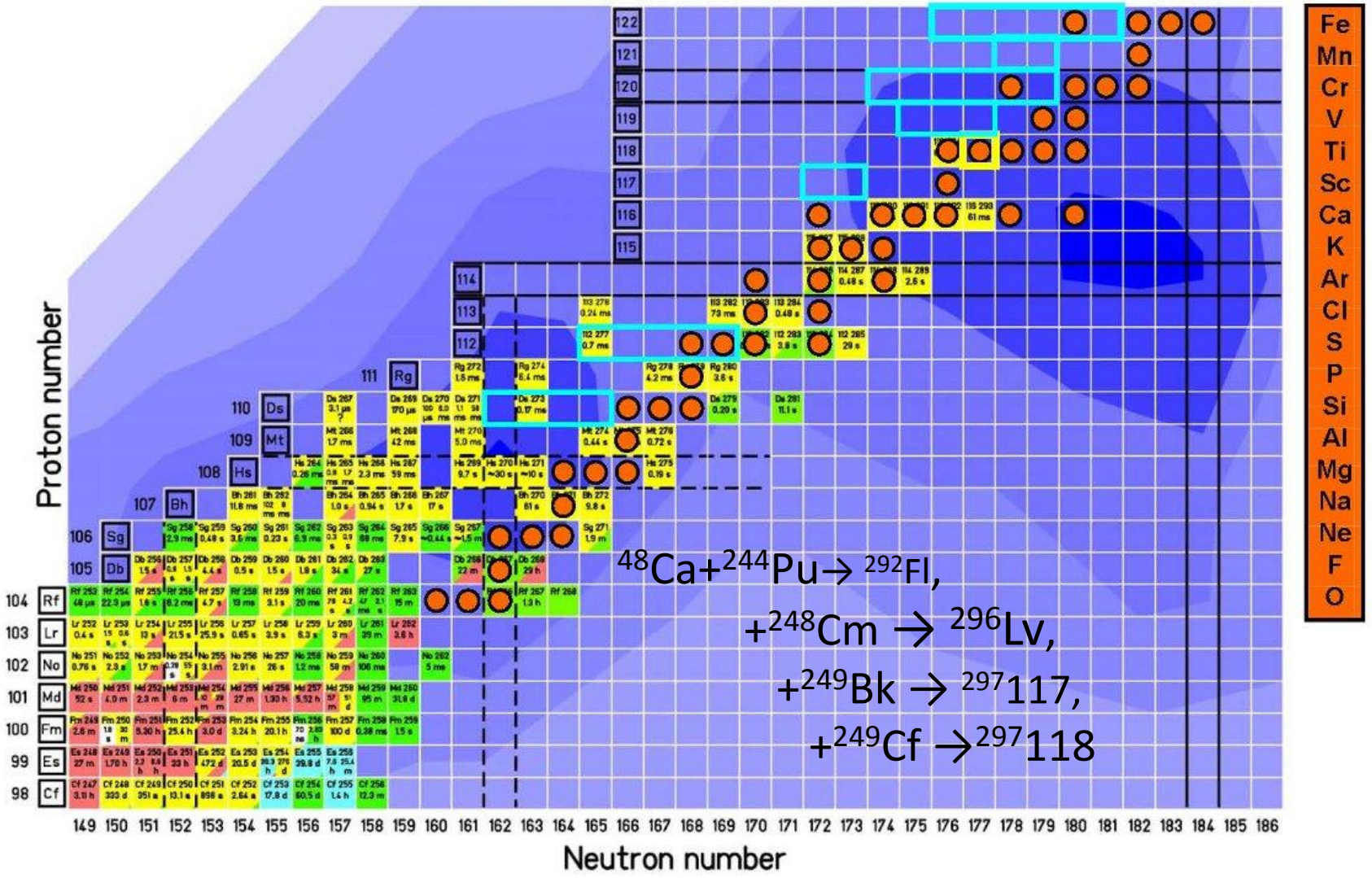

About synthesis of super heavy elements

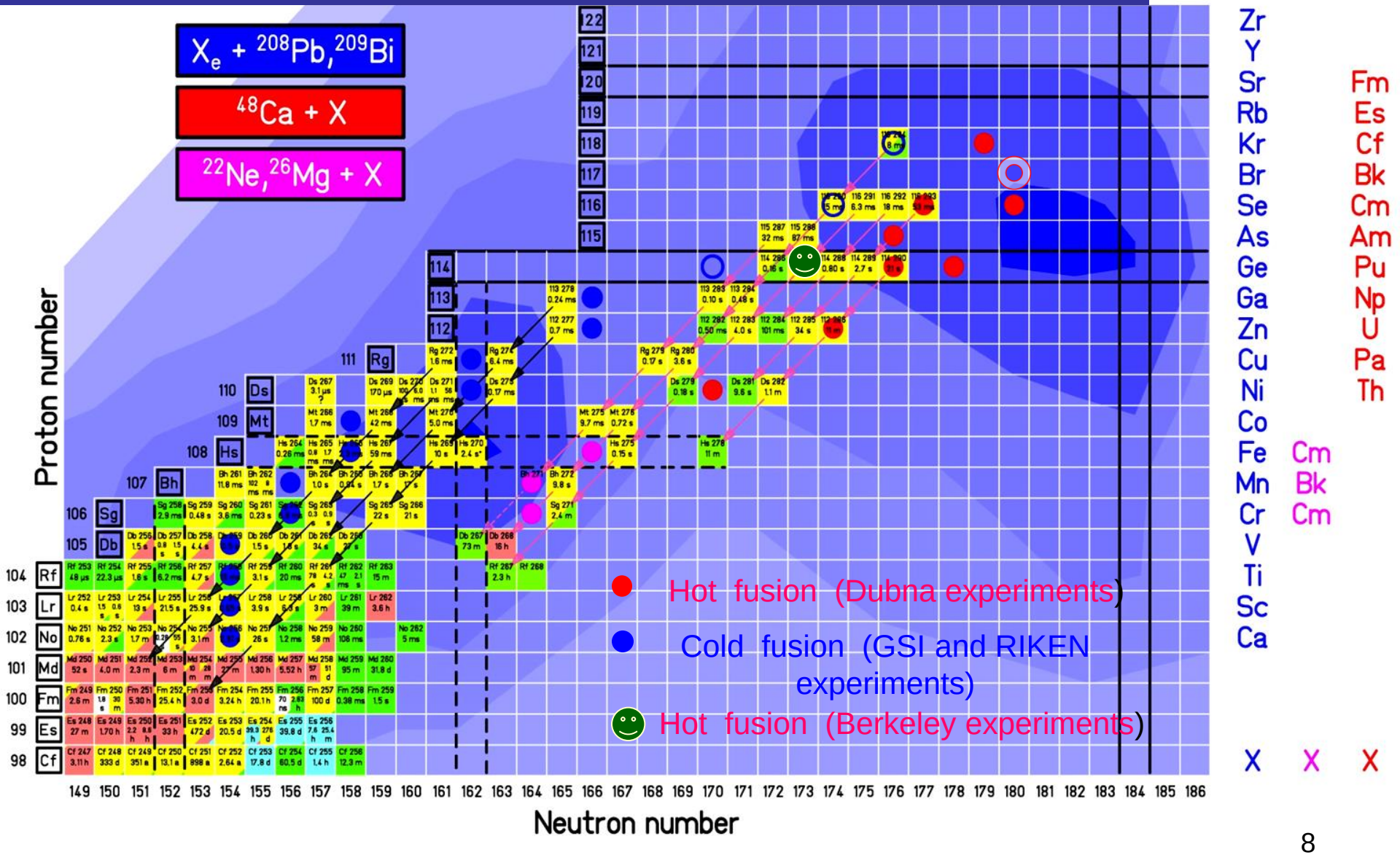

The Origin of the Nuclear Energy.

Exothermic Chemical Reactions

Heat is evolved in the chemical reaction in which hydrogen and oxygen are combined to be water;

i.e. th reaction in which heat i e chemical equat n is written

Name kJ of heat is evolved. Anoth

where one mol of carbon is oxidated t o be carbon dioxide with producing 394 kJ of heat.

Heat at burning of hydrogen and carbon

The above chemical equations, (1) and (2), are for one mol of hydrogen and carbon, respectively. In order to compare these chemical reactions with nuclear reactions, it is convenient to rewrite these equations "for one molecule". For this, let us divide the heat production by the Avogadro constant

$$N_{\mathrm{A}} = 6.02 \times 10^{23}\ \mathrm{mol}^{-1} \qquad 1\,\mathrm{eV} = 1.60 \times 10^{-19}\ \mathrm{J}$$

Then they are rewritten as

$$\mathrm{H_2} + \frac{1}{2}\,\mathrm{O_2} \rightarrow \mathrm{H_2O} + 3.0\,\mathrm{eV} \qquad (3)$$

$$\mathrm{C} + \mathrm{O_2} \rightarrow \mathrm{CO_2} + 4.1\,\mathrm{eV} \qquad (4)$$

Equation (3) means that the process in which two hydrogen and one oxygen molecules combine to be one water molecule generates 3.0 eV energy emission. And Eq. (4) says that, when a carbon atom combines with an oxygen molecule to be a carbon dioxiside molecule, 4.1 eV energy is released.

As learned before, **eV** is a unit of energy extensively used in the atomic and nuclear world. It is the work done on an electron that is accelerated through a potential difference of one volt. Its value is

We can understand that **"the energy evolved from one process of an exothermic chemical reaction is about 3 or 4 eV"**.

Exothermic Nuclear Reactions

Nuclei show various types of reaction: For example, one nuclide splits into two or more fragments. This type of reaction is called **nuclear fission**.

Contrarily, two nuclides sometimes combine with each other to be a new nuclide. This type of reaction is called **nuclear fusion**.

There are many other types of reaction processes; they are generally called **nuclear reactions**.

Among these various types of nuclear reactions, there are some types of exothermic reactions which are sometimes called "**exoergic**" reaction in nuclear physics.

Cold fusion-fission reaction

First controlled 'atom smasher' experiment by Cockcroft and Walton.

$$ {}^{1}_{1}\mathrm{p} + {}^{7}_{3}\mathrm{Li} \rightarrow {}^{4}_{2}\mathrm{He} + {}^{4}_{2}\mathrm{He} $$

Q=17.3 MeV.

m_p=7.289 MeV, m_{Li}=14.908 MeV, m_{He}=2.424 MeV

Incoming proton had energy of 0.125 MeV.

First direct experimental check of $E=mc^2$

Exothermic reactions

Where is the exothermic heat energy coming from?

The heat comes from the energy stored in the nuclear binding energies of the reactant nuclei. The binding energies of initial nuclei are greater than the energy stored in the binding energies of the reaction products.

In endothermic reactions, the situation is reversed: more binding energy is stored in the reaction products than in the reactants nuclei.

Exothermic Nuclear Reactions

The nucleus of deuterium atom is called **deuteron** which consists of a proton and a neutron. It is represented by a symbol **"d"**. The nuclear reaction in which two deuterons bind with each other is an example of nuclear **fusion**. This exoergic reaction is written as

$$\mathrm{d} + \mathrm{d} \rightarrow {}^{3}_{2}\mathrm{He} + \mathrm{n} + 3.27\,\mathrm{MeV} \qquad (5)$$

If a neutron is absorbed in the uranium-235 nucleus, it would split into two fragments of almost equal masses and evolves some number of neutrons and energy *Q*. One of the equations for the processes is written

$${}^{235}_{92}\mathrm{U} + \mathrm{n} \rightarrow {}^{137}_{56}\mathrm{Ba} + {}^{97}_{36}\mathrm{Kr} + 2\,\mathrm{n} + Q \qquad (6)$$

This is an example of nuclear **fission**.
Here it is quite interesting how much the amount of the energy emission *Q* is. It must be about 200 MeV.

$$\mathrm{H_2} + \frac{1}{2}\,\mathrm{O_2} \rightarrow \mathrm{H_2O} + 3.0\,\mathrm{eV} \qquad (3)$$

$$\mathrm{C} + \mathrm{O_2} \rightarrow \mathrm{CO_2} + 4.1\,\mathrm{eV} \qquad (4)$$

The nuclear reaction energy is million times more than energy of chemical reactions !

Nuclear Power in the World Today

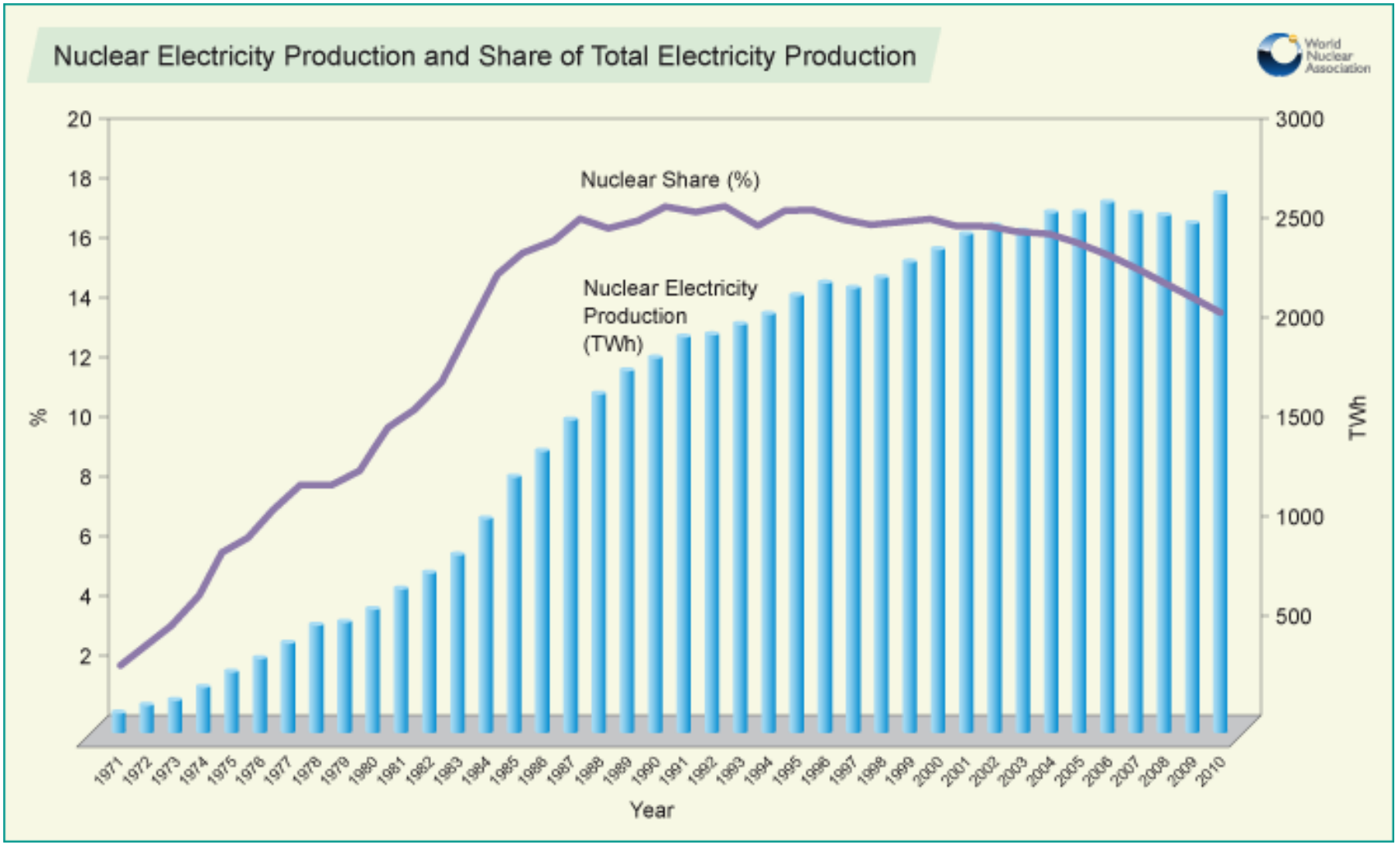

Part of the nuclear power stations in world electricity production.

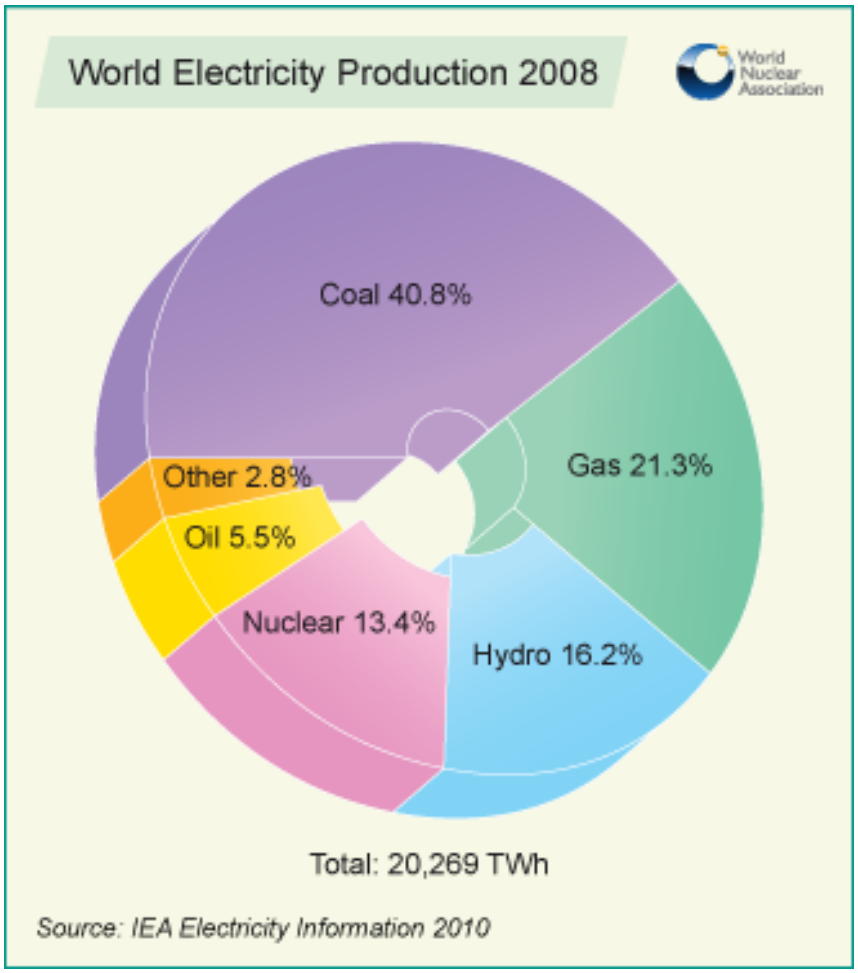

Over 60 further nuclear power reactors are under construction, equivalent to 17% of existing capacity, while over 150 are firmly planned, equivalent to 48% of present capacity.

Fuel for Electricity Generation 2008

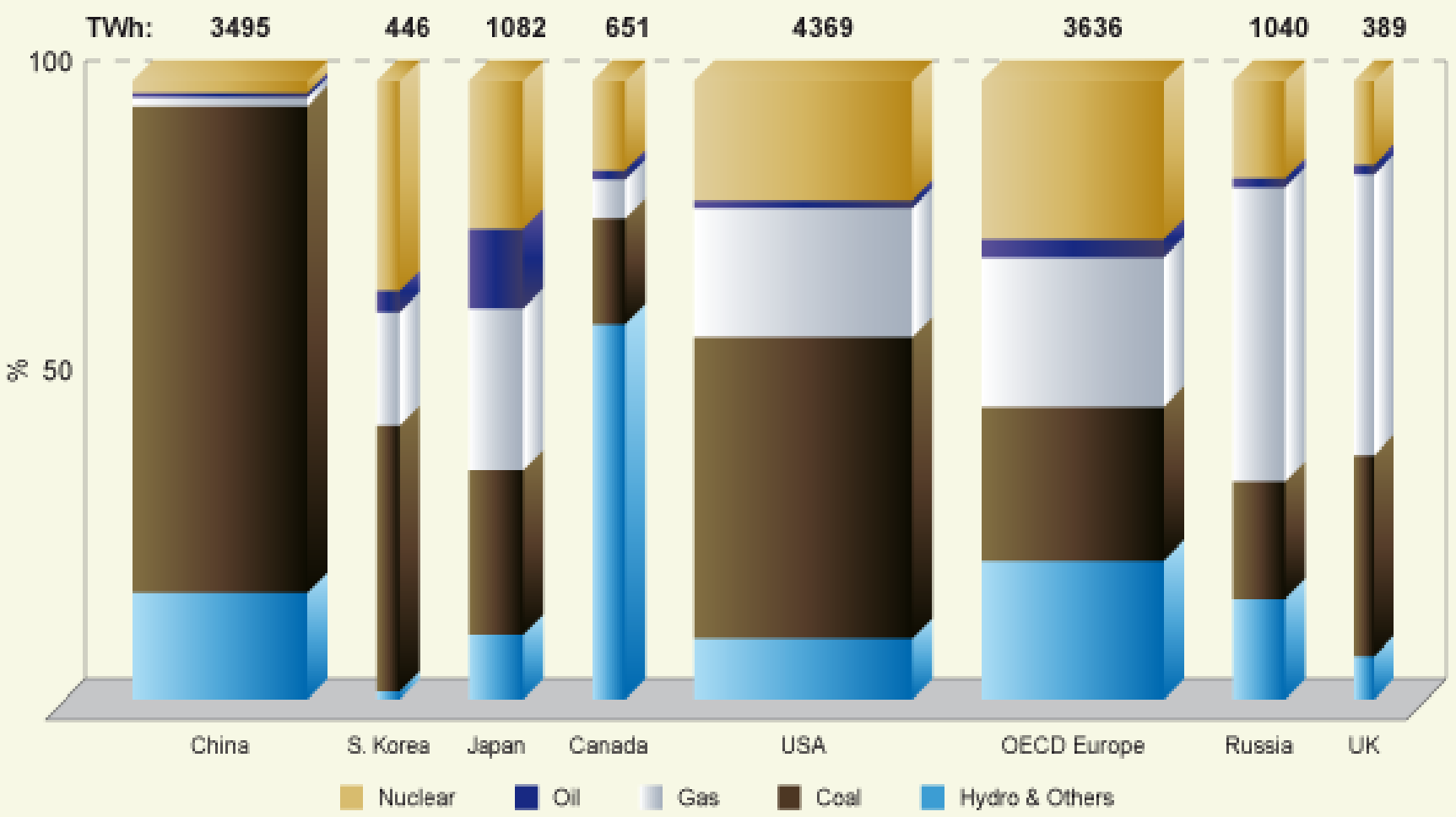

Width of each bar is indicative of gross power production

Main Source: OECD/IEA Electricity Information 2010

Nuclear Electricity Generation

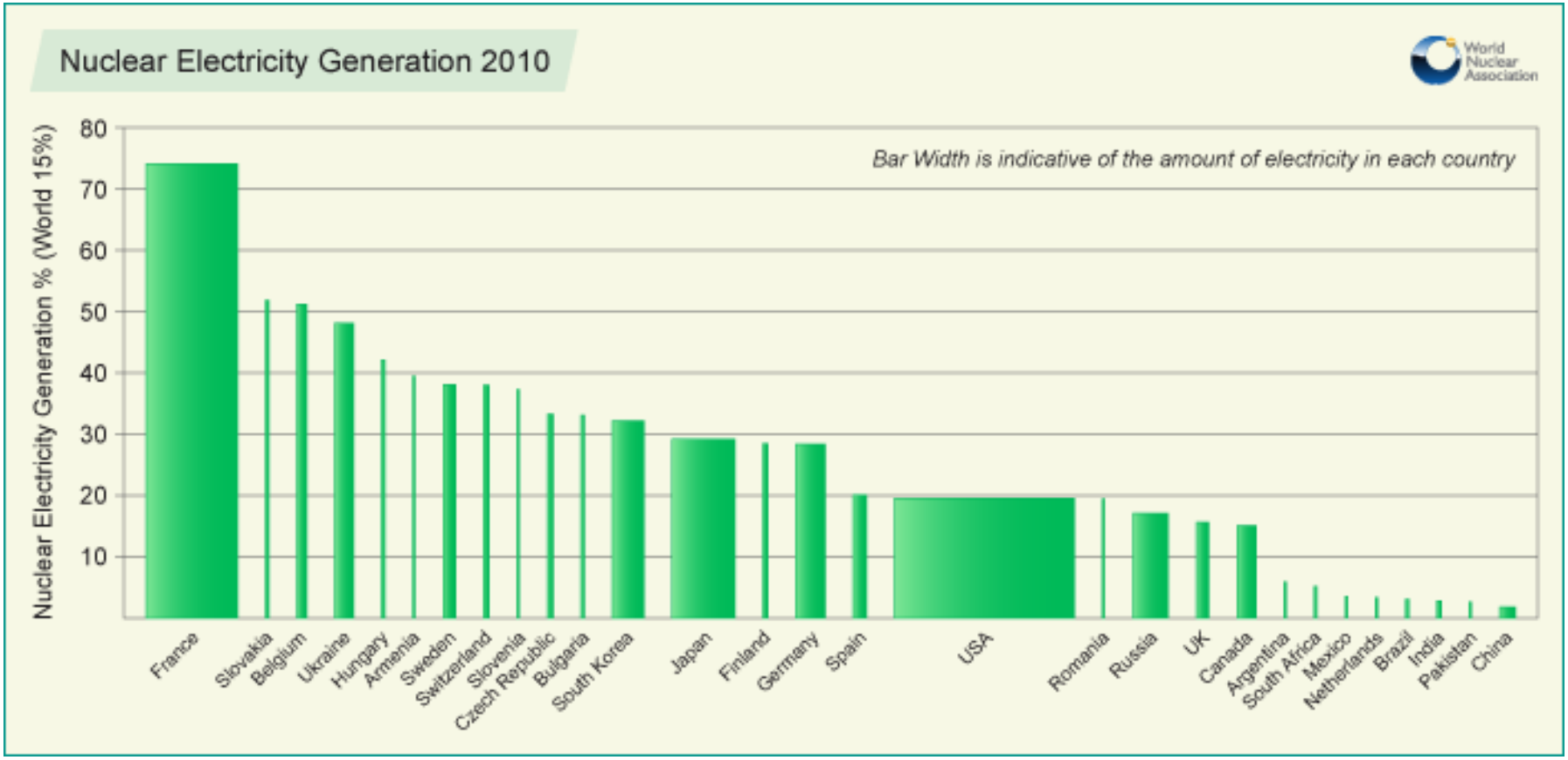

Analogies of four basic chemical and nuclear reactions types: synthesis, decomposition, single replacement and double replacement.

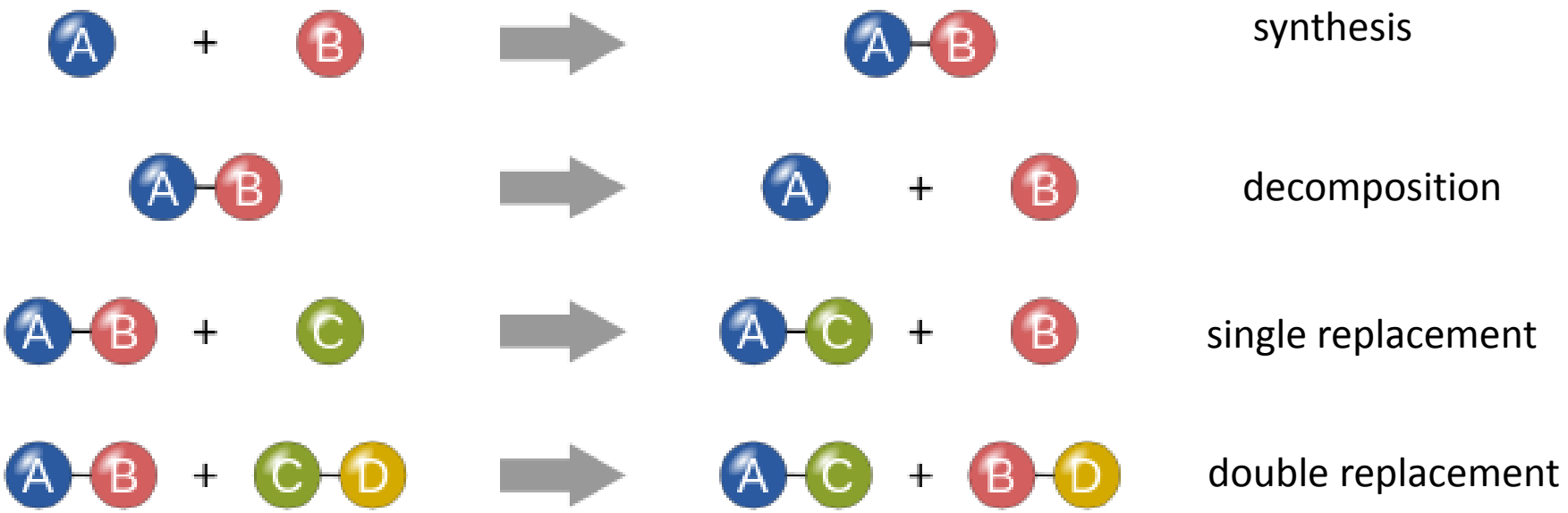

Sources of atomic energy

- An absorption or release of nuclear energy occurs in nuclear reactions or radioactive decay.
- Those that absorb energy are called endothermic reactions and those that release energy are exothermic reactions. Energy is consumed or liberated because of differences in the nuclear binding energy between the incoming and outgoing products of the nuclear reactions.
- The best-known classes of exothermic nuclear transmutations are fission and fusion. Nuclear energy may be liberated by atomic fission, when heavy atomic nuclei (like uranium and plutonium) are broken apart into lighter nuclei. The energy from fission is used to generate electric power in hundreds of locations worldwide.
- Nuclear energy is also released during atomic fusion, when light nuclei like hydrogen are combined to form heavier nuclei such as helium. The Sun and other stars use nuclear fusion to generate thermal energy which is later radiated from the surface, a type of stellar nucleosynthesis.
- In order to quantify the energy released or absorbed in any nuclear transmutation, one must know the nuclear binding energies of the nuclear components involved in the transmutation.

Mechanism of releasing nuclear energy.

Reaction energy balance $\boldsymbol{Q}$ is determined by mass difference between the initial and final sets of particles

$$Q = \Delta m c^2 = \left(m_{\mathrm{a}} + m_{\mathrm{X}} - m_{\mathrm{Y}} - m_{\mathrm{b}}\right)c^2$$

a) If $\boldsymbol{Q}$ > 0, reaction is *exothermic* (energy released as kinetic energy and g-rays).

b) If $\boldsymbol{Q}$ <0, reaction is *endothermic.* There is a threshold of the energy of the incoming particle to make the reaction happen.

c) $\boldsymbol{Q}$ =0 is elastic scattering. Total kinetic energy is conserved

Why is energy released during fission ?

$$ {}^{1}_{0}n + {}^{235}_{92}U \rightarrow {}^{236}_{92}U^{*} \rightarrow {}^{144}_{56}Ba + {}^{89}_{36}Kr + 3{}^{1}_{0}n $$

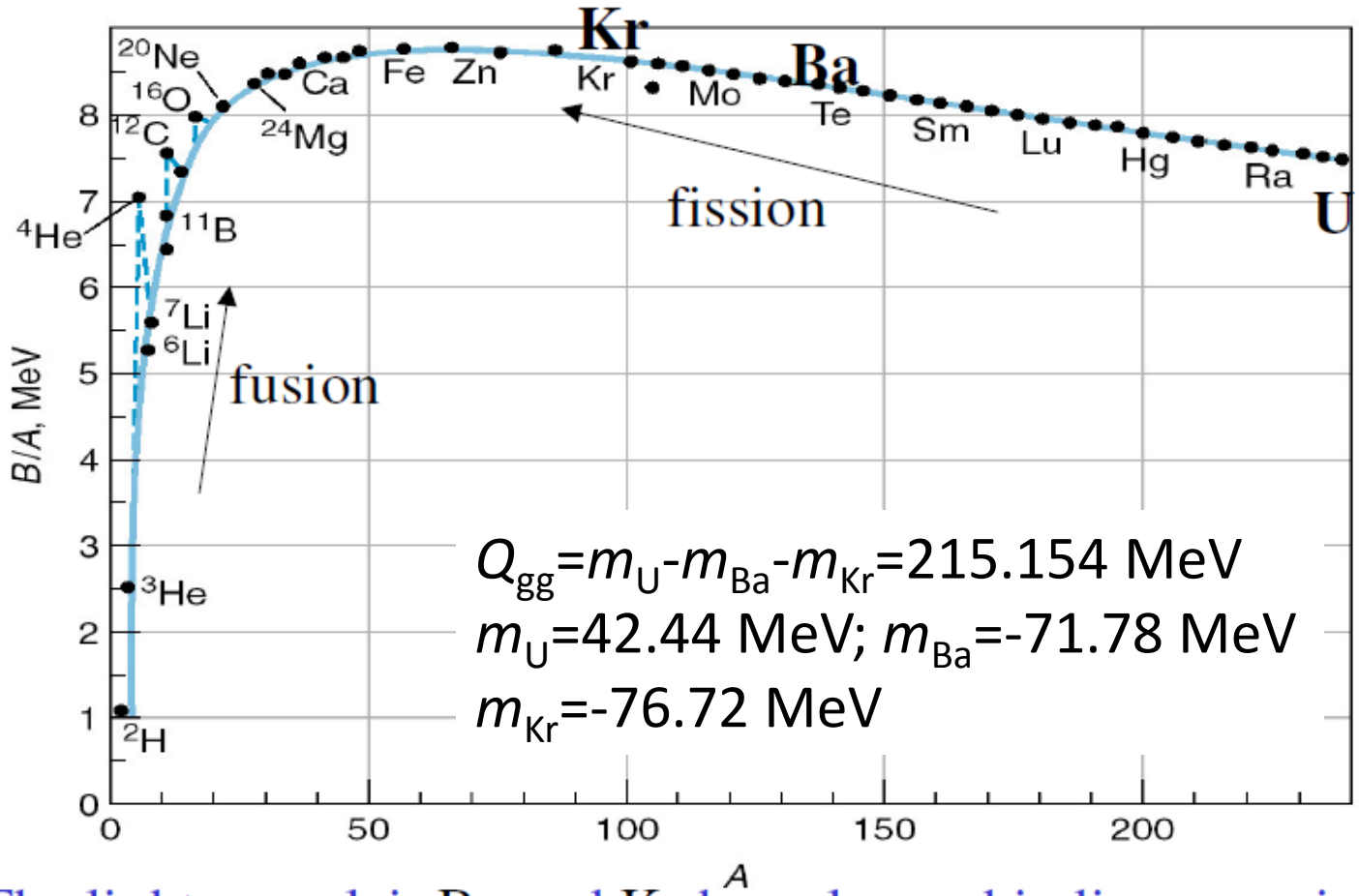

$Q_{gg}=m_U-m_{Ba}-m_{Kr}=215.154$ MeV

$m_U=42.44$ MeV; $m_{Ba}=-71.78$ MeV

$m_{Kr}=-76.72$ MeV

The lighter nuclei: Ba and Kr have larger binding energies/nucleon than U

Mass excess, binding energy and energy balance

Mass excess $\Delta m(A,Z)=M(A,Z)-A\cdot u$

M(A,Z) is the mass of nucleus and A is its mass number.; u is mass units

$u=M_{12C}/12=931.494$ MeV; or $u= 1660538.73(0.13)10^{-33}kg$

$M_p=7.289$ MeV; $M_n=8.071$ MeV;

Binding energy $B=\Delta m(A,Z)-Z\cdot M_p -N\cdot M_n$

$\Delta m_U=42.44$ MeV; $B_U/A= 7.586$

$B_U=42.44-92\cdot7.289-144\cdot8.071=-1790.372$ MeV;

$\Delta m_{Ba}=-71.78$ MeV; $B_{Ba}/A= 8.265$

$B_{Ba}=-71.78-56\cdot7.289-88\cdot8.071=-1190.212$ MeV;

$\Delta m_{Kr}=-76.72$ MeV; $B_{Kr}/A= 8.617$

$B_{Kr}=-76.72-36\cdot7.289-53\cdot8.071=-766.887$ MeV;

Energy balance in nuclear fission $^{236}U \rightarrow {}^{144}Ba+{}^{89}Kr$ channel:

$Q_{gg}=m_U-m_{Ba}-m_{Kr}=215.154$ MeV

Fission Energy Distribution

In the fission process, the fragments and neutrons move away at high speed carrying with them large amounts of kinetic energy.
The neutrons released during the fission process are called fast neutrons because of their high speed. Neutrons and fission fragments fly apart instantaneously in a fission process.

- Gamma rays (photons) equivalent to 8 MeV of energy are released within a microsecond of fission.
- The two fragments are beta emitters. Recall that beta decays are accompanied by antineutrino emissions, and the two types of particles carry away approximately equal amounts of energy.

Estimated average values of various energies are given in a table:

Energy (MeV) distribution in fission reactions	
Kinetic energy of fission fragments	167 MeV
Prompt (< 10-6 s) gamma ray energy	8
Kinetic energy of fission neutrons	8
Gamma ray energy from fission products	7
Beta decay energy of fission products	7
Energy as antineutrinos (ve)	7

The neutron with the thermal energy (E_n= 0,025 eV) causes excitation and fission of atomic nuclei

Fission Chain Reaction

1 neutron goes in, 2-3 neutrons go out! They can also go on to induce fission

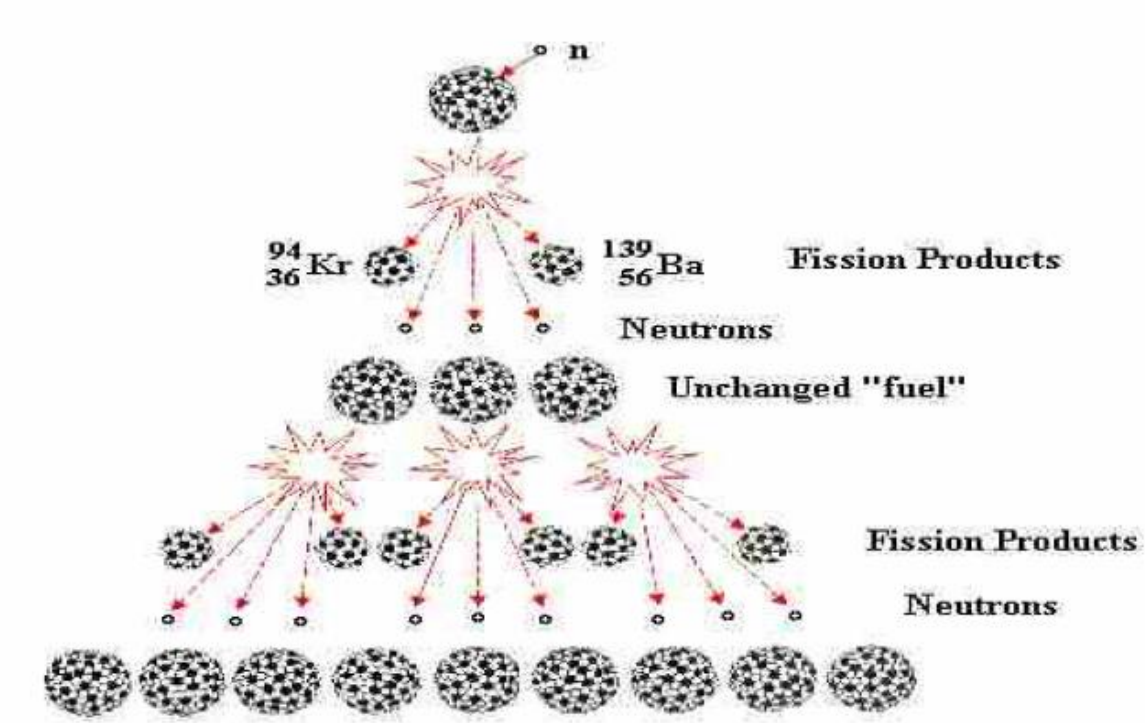

Critical mass needed to allow process to increase with time.
Depends on material, geometry, and apparatus.
Used in nuclear reactors and bombs!

The neutron with the thermal energy (E_n= 0,025 eV) causes excitition and fission of atomic nuclei

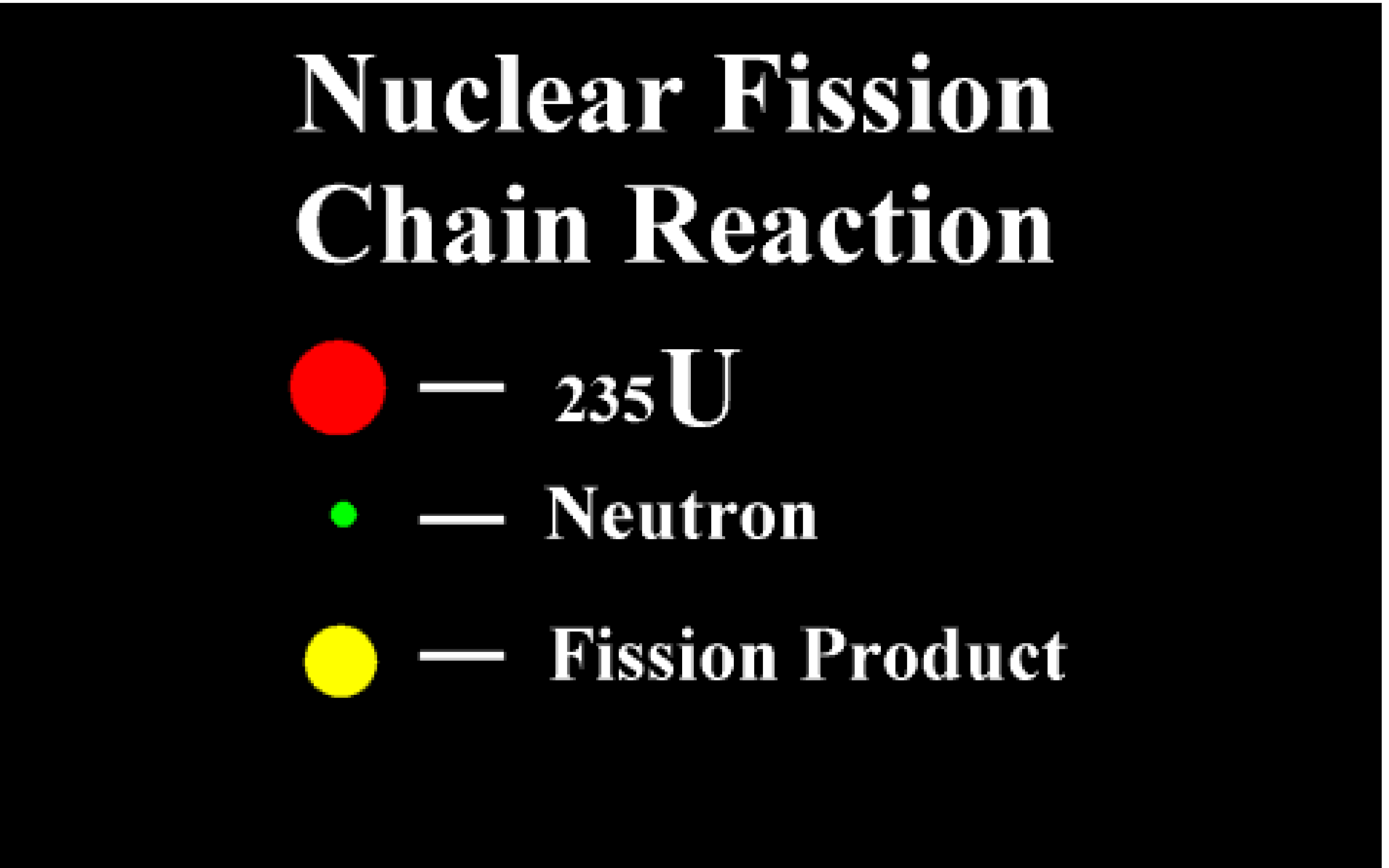

Experimental results to study fission mechanism and role of the nuclear structure

In the experiment they measure kinetic energy and velocity, angular distributions of the fragments, neutron multiplicity and energy spectra, as well as gamma multiplicity accompanying fission fragments.

Experimental setup CORSET

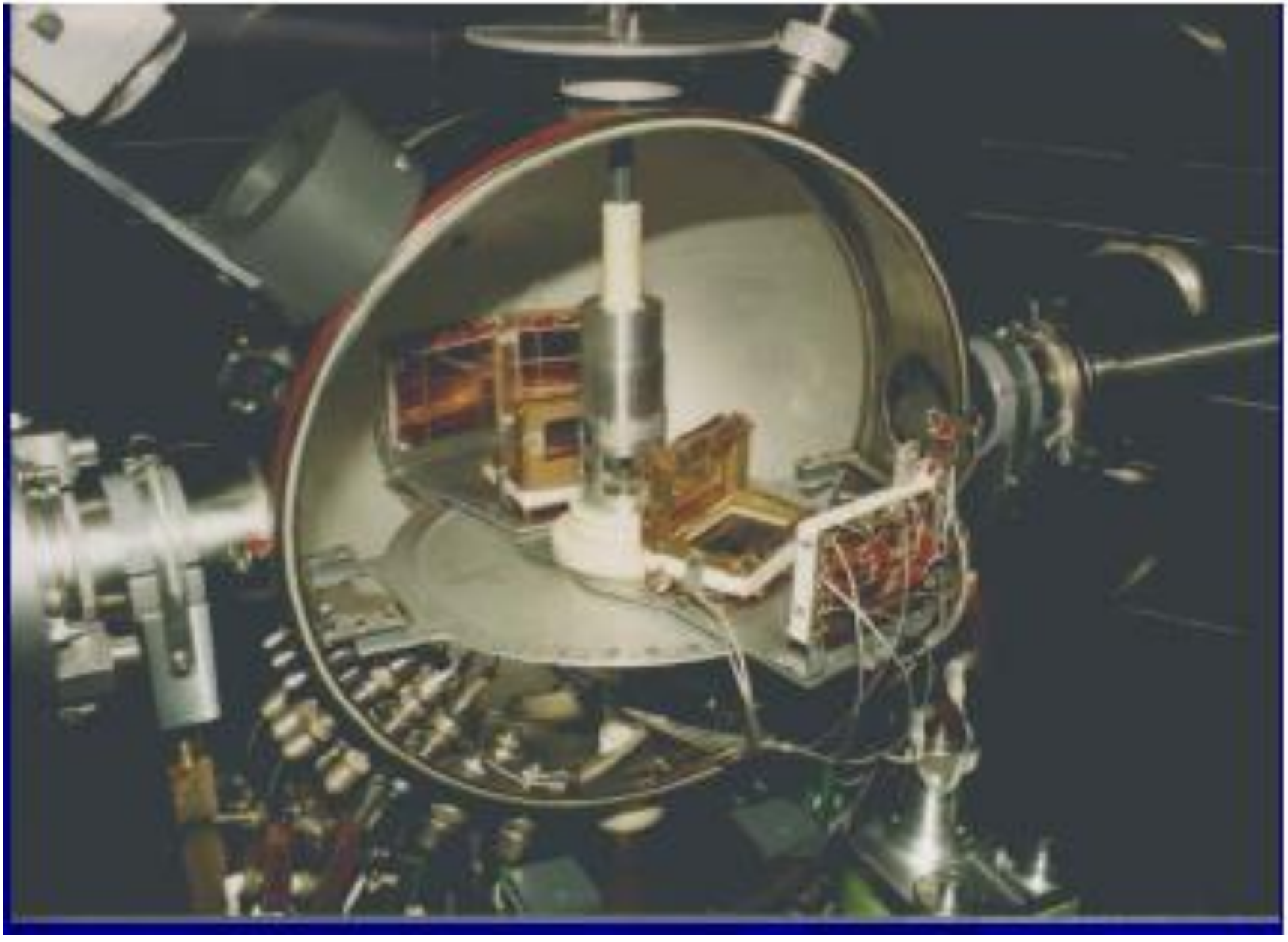

CORSET setup

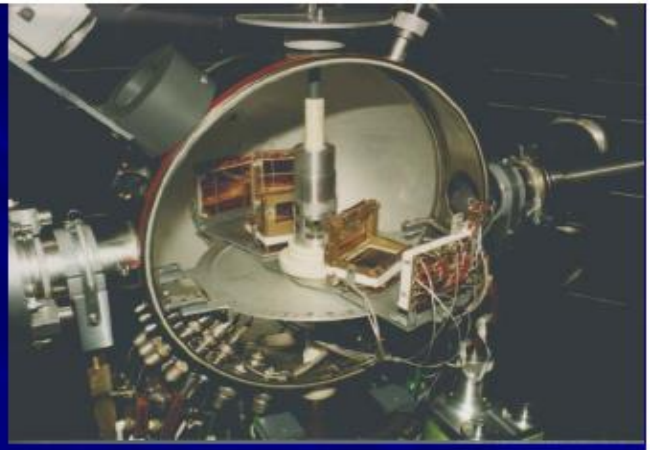

position sensitive
stop detector
x, y, TOF

F_1

TOF-start
detector

TOF-start
detector

mass
resolution – 2 a.m.u

Beam
P

Target

^{232}Th,
^{238}U,^{242}Pu

F_2

angular
resolution – 0.3^0

solid angle – 0.3 sr

Both fission products are registered in coincidence.

Fission of nuclei

1. Spontaneous fission;

2. Fission induced by neutrons, gamma quantum, protons;

3. Fusion-fission reactions;

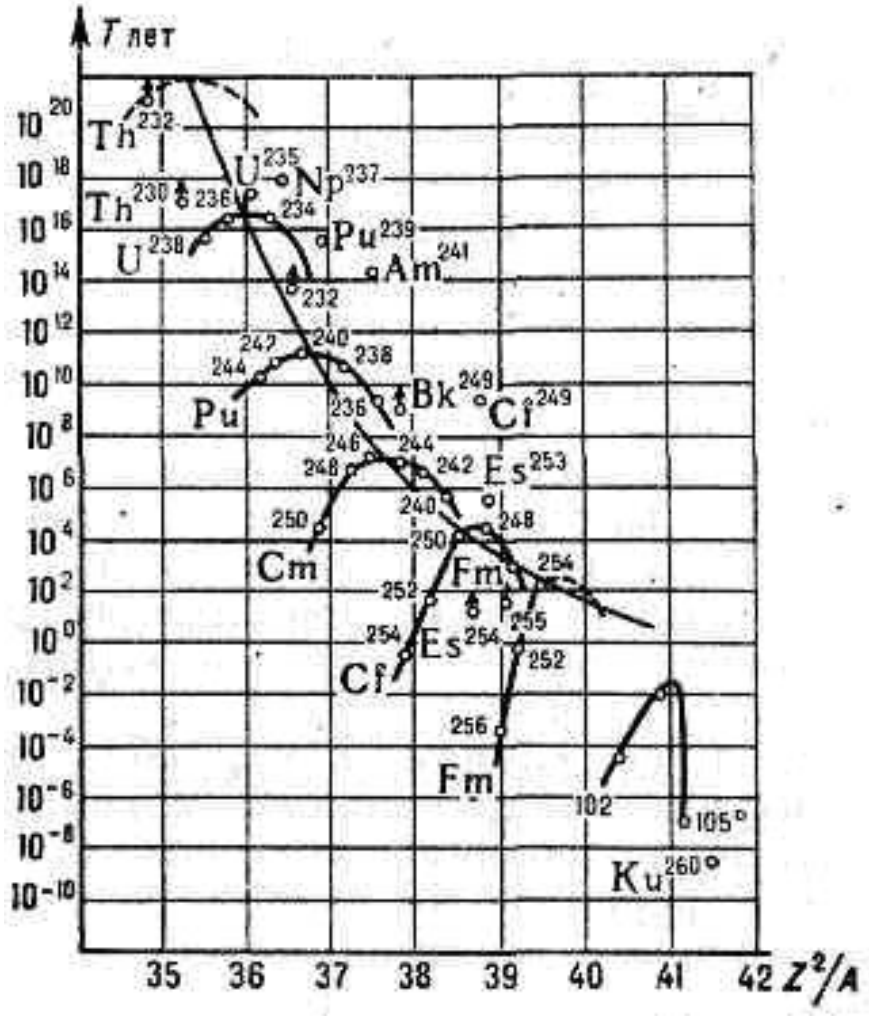

Fission induced by protons

A=N+Z

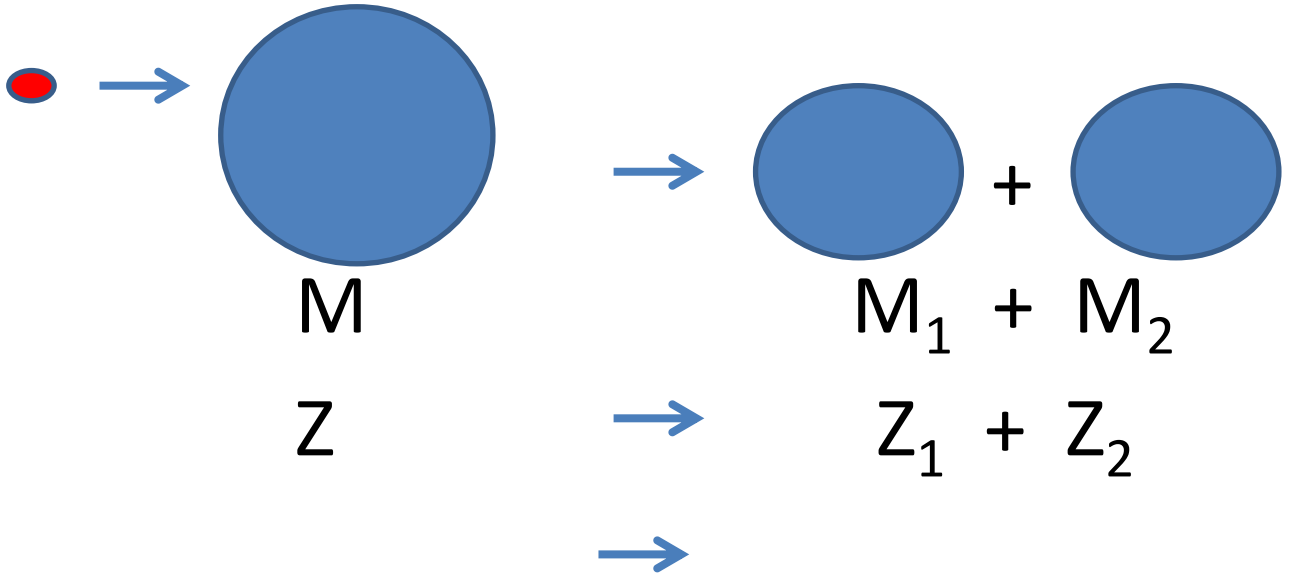

$$Q_{gg} = (M_1 + M_2 - M)c^2 \rightarrow E_p + Q_{gg} > \frac{M_1 v_1^2}{2} + \frac{M_2 v_2^2}{2}$$

The source of the kinetic energy of products is intrinsic binding energy of system

Spontaneous fission properties and lifetime systematics.

Nucl.Phys. A502 (1989) 21c40c.

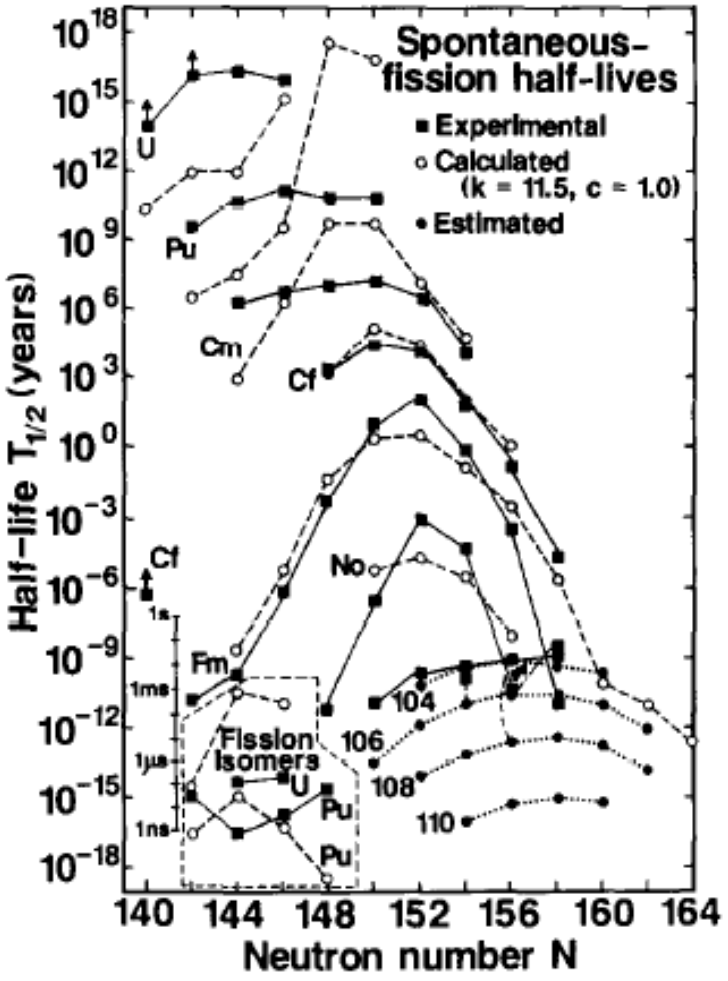

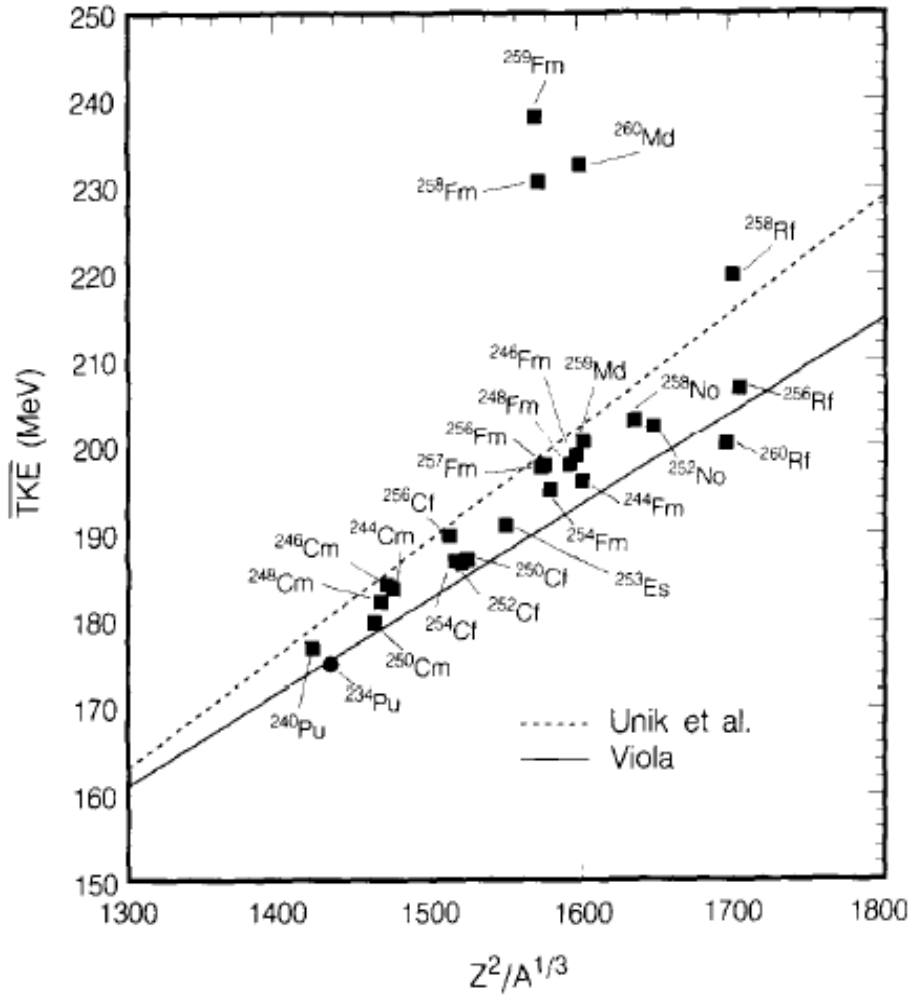

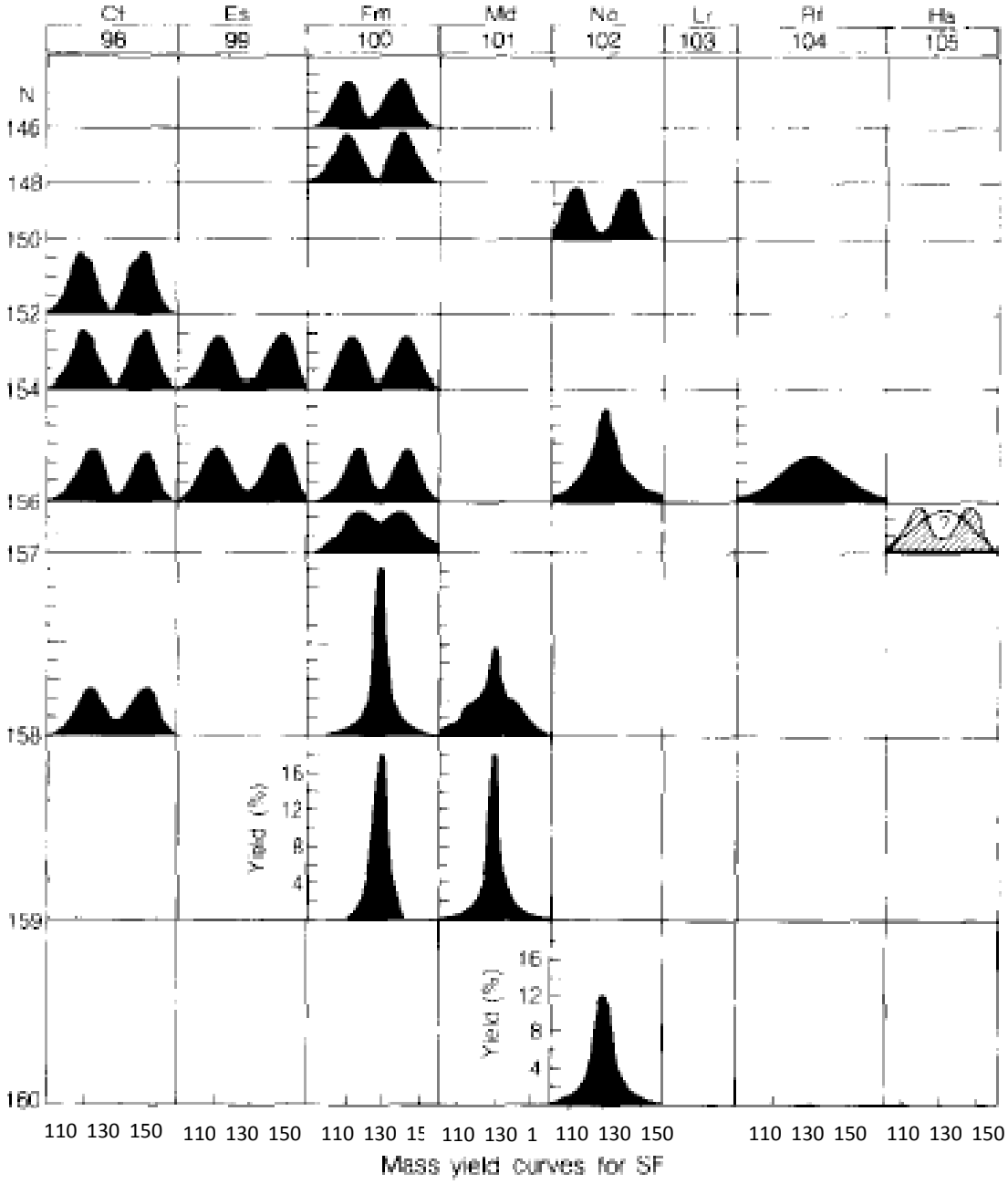

Asymmetric and Symmetric mass distributions of fission products as a function of the neutron numbers.

Mass and total energy distribution of the fission fragments.

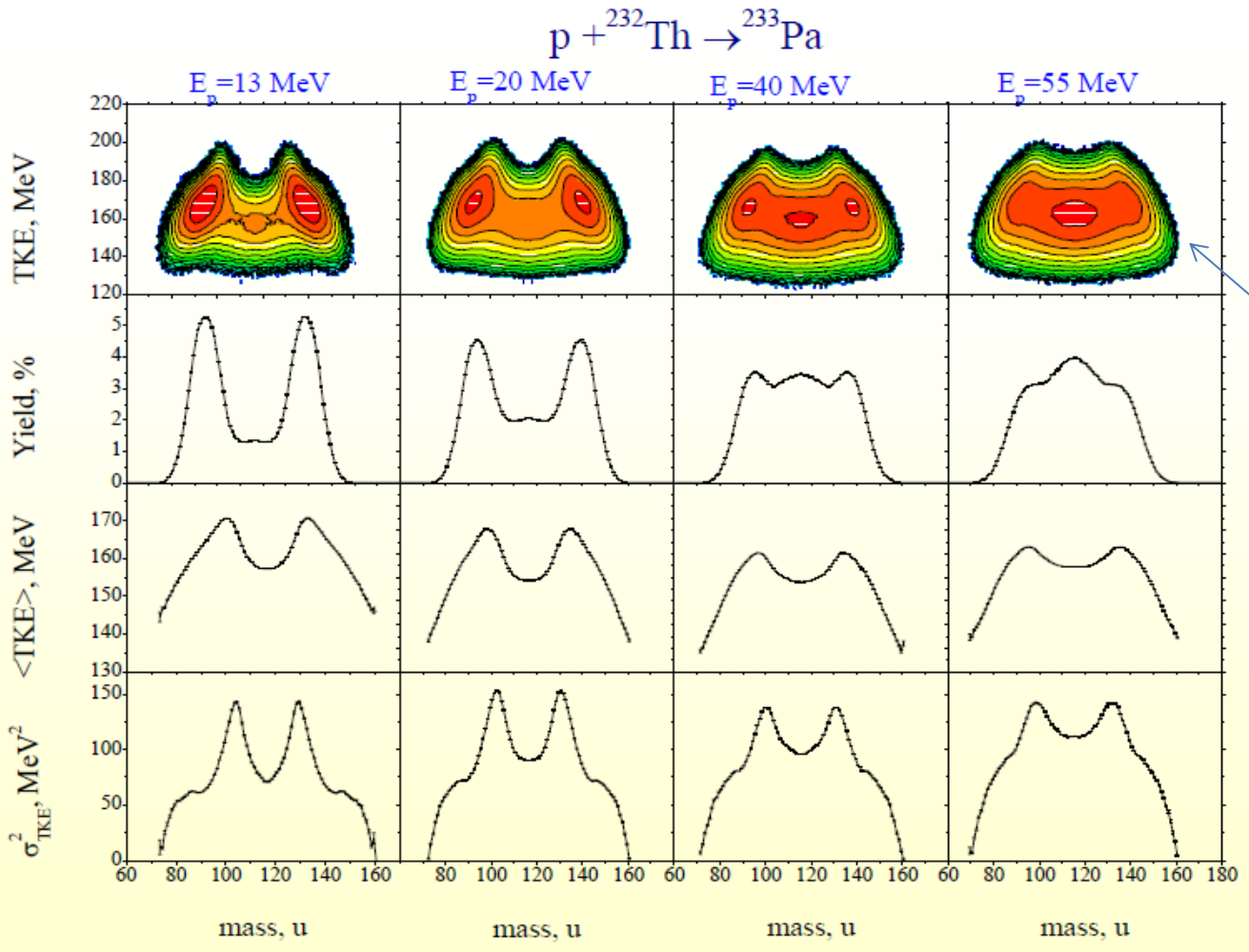

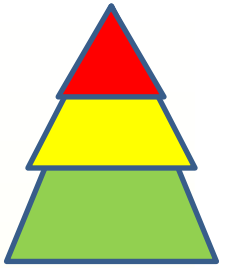

Prpjection of 3D figure

From top to bottom: two dimensional mass-TKE matrices, mass distribution of fission fragments, average TKE and square variance of TKE as a function of fission fragment mass at the proton energies 13, 20, 40 and 55 MeV

Mass distribution of the fission products as a function of the excitation energy of compound nucleus

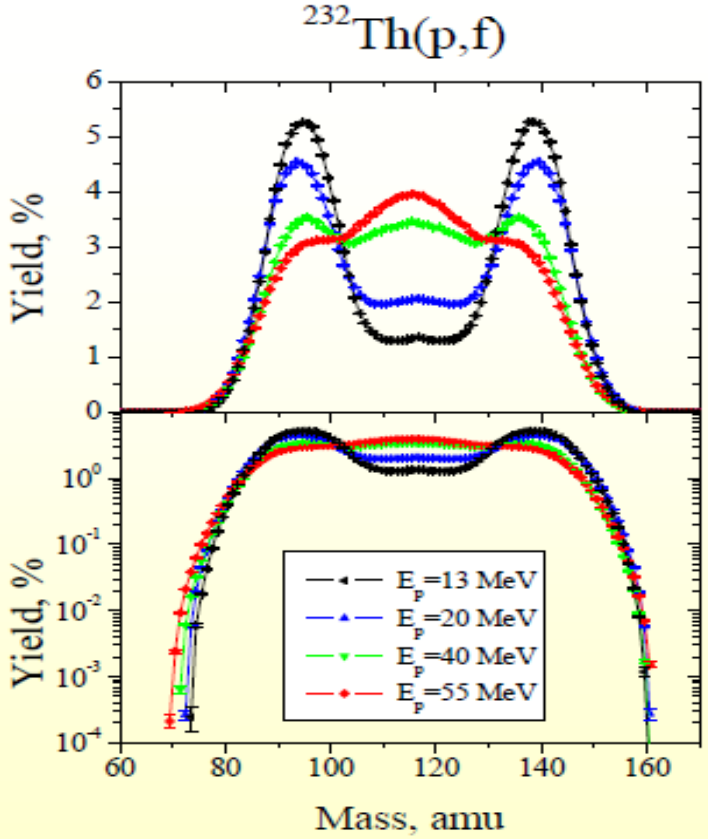

The mass distribution in linear and logarithmic scale for the proton-induced fission of ^{232}Th at the proton energies 13, 20, 40 and 55 MeV

5.5 LIQUID-DROP DEFORMATION ENERGY

The basic ideas of the liquid drop model are described in Chapter 4. The binding energy is given by

$$B_{LD}(N,Z) = b_V A\left[1 - K_V\left(\frac{N-Z}{A}\right)^2\right] - b_S A^{2/3}\left[1 - K_S\left(\frac{N-Z}{A}\right)^2\right]$$
$$-b_C\frac{Z^2}{A^{1/3}} + \delta\left[(-1)^N + (-1)^Z\right]A^{-1/2}. \qquad (4.3.2)$$

for a spherical nucleus. When the nucleus assumes a deformed shape, its surface area must be larger, since the sphere has the smallest area for a given volume. Thus the surface-energy term proportional to $A^{2/3}$ will increase by a factor $S_0 > 1$, the ratio of the area of the deformed nucleus to that of the sphere. Similarly, a deformed nucleus will have a smaller Coulomb energy, because it is less compact and the charges lie farther from one another; thus the Coulomb energy will decrease by a factor $C_0 \leq 1$ compared to the spherical shape. Including these factors, we find

$$B_{LD} = b_V A\left[1 - K_V\left(\frac{N-Z}{A}\right)^2\right] - b_S A^{2/3}\left[1 - K_S\left(\frac{N-Z}{A}\right)^2\right]S_0$$
$$-b_C\frac{Z^2}{A^{1/3}}C_0 + \delta\left[(-1)^N + (-1)^Z\right]A^{-1/2}. \qquad (5.5.1)$$

Nuclear binding energy in the liquid drop model

The factors S_0 and C_0 may be easily found using the surface defined by eq. (5.3.1) with all $m=0$ (i.e. axial symmetry). The surface area is

$$S = 2\pi \int_0^{\pi} R^2(\theta) \sin\theta \sqrt{1 + \frac{1}{R^2}\left(\frac{dR}{d\theta}\right)^2}\, d\theta \tag{5.5.2}$$

which to second order in the deformation parameters $\alpha_{\ell m}$ results in [Bohr and Wheeler]

$$S = 4\pi R^2(A) S_0 = 4\pi R^2(A)\left[1 + \frac{1}{8\pi}\sum_{\ell=2}(\ell-1)(\ell+2)\alpha_{\ell 0}^2\right]. \tag{5.5.3}$$

The Coulomb energy of a uniformly charged drop of density n is

$$E_C = \frac{1}{2} n^2 \int\int_{vol} \frac{d^3\vec{r}_1 d^3\vec{r}_2}{|\vec{r}_1 - \vec{r}_2|} \tag{5.5.4}$$

which for the shape in eq. (5.3.1) can be calculated to second order in the $\alpha_{\ell m}$. We find

$$E_C = \frac{3}{5}\frac{Z^2 e^2}{R(A)} C_0 = \frac{3}{5}\frac{Z^2 e^2}{R(A)}\left[1 - \frac{5}{4\pi}\sum_{\ell=2}\frac{\ell-1}{2\ell+1}\alpha_{\ell 0}^2\right]. \tag{5.5.5}$$

Deformation energy in the liquid drop model

then

$$E_D = \sum_{\ell=2} C_\ell \alpha_{\ell 0}^2 \equiv \sum_{\ell=2} \frac{(\ell-1)}{8\pi} \alpha_{\ell 0}^2 \left[\ell + 2 - \frac{20x}{2\ell+1}\right] \tag{5.5.6}$$

where the fissility parameter x is defined by

$$x = \frac{b_C}{2b_S} \frac{Z^2}{A\left[1 - K_S\left(\frac{N-Z}{A}\right)^2\right]} \equiv \frac{Z^2/A}{(Z^2/A)_c}. \tag{5.5.7}$$

When C_ℓ is positive (negative), the nucleus is stable (unstable) against deformations of the type $\alpha_{\ell 0}$. Thus the nucleus is least stable against deformations of smallest multipole order. In fact $C_2 > 0$ if and only if $x < 1$. This is the reason for the definition of $(Z^2/A)_c$, where c means critical.

Mass distribution of the fission products obtained by liquid drop model is symmetric because minimum values of the potential energy surface calculated by this model correspond to the mass symmetric region.

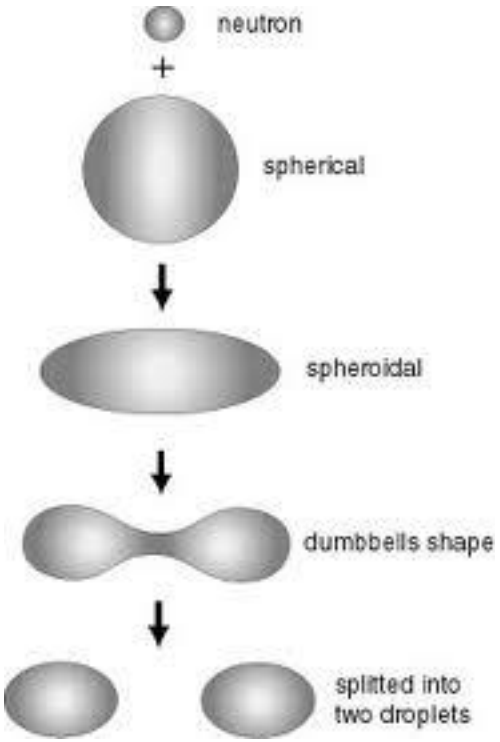

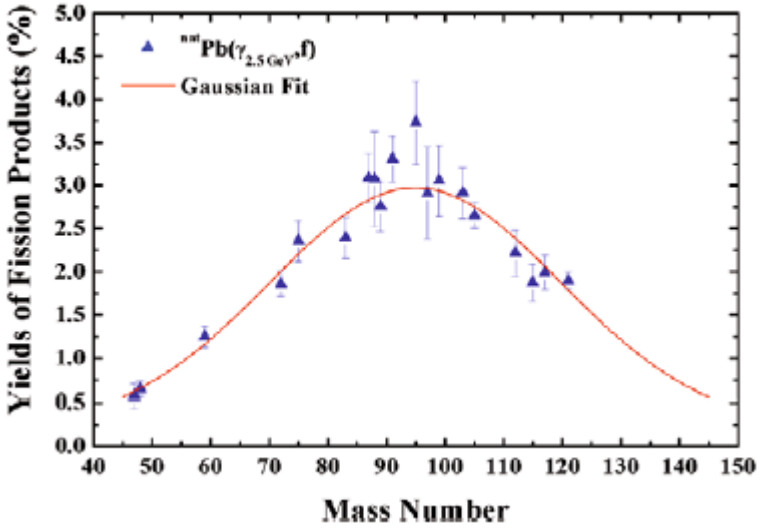

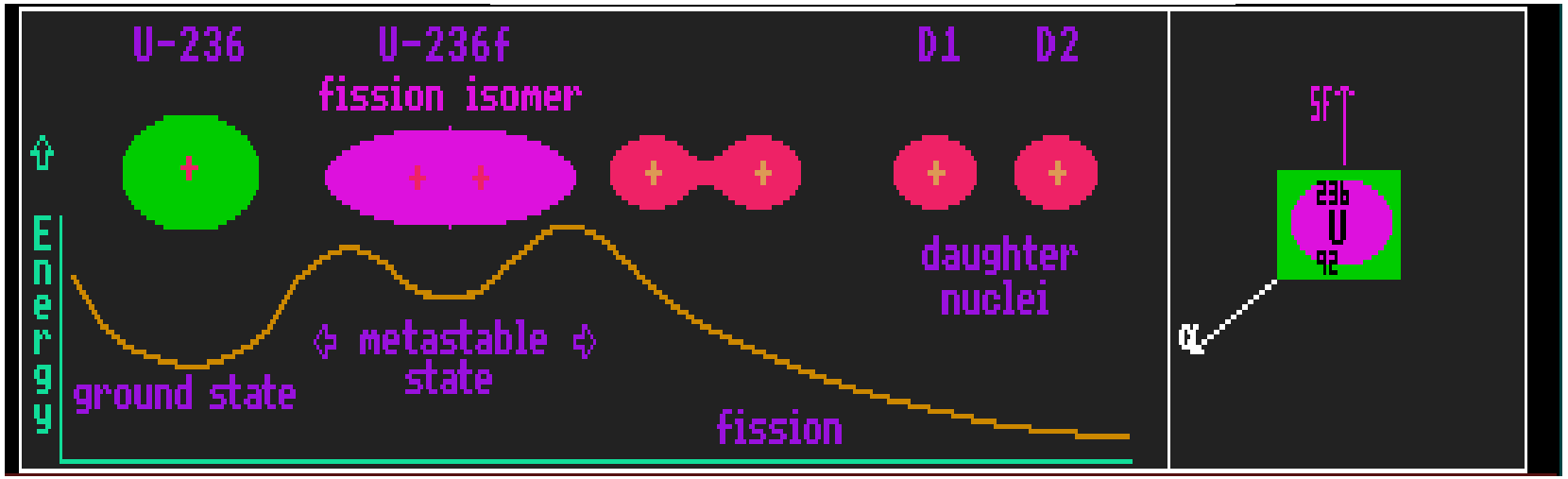

Note,

1) two center shape of the mass and charge distributions are appearance of the shell structure of being formed fragments;

2) Transition of the shape of the mass and charge distributions from the two center shape in one center symmetric shape means the decreasing of the shell effects by increasing the effective temperature of interacting nuclei. Fluctuation energy of nucleons becomes comparable and large than distance between energy levels.

$$\Gamma_i = \frac{\hbar}{\tau_i} = \frac{\sqrt{2}\pi}{32\hbar\varepsilon_{F_K}^{(\alpha)}}\left[(f_K - g)^2 + \frac{1}{2}(f_K + g)^2\right]$$

$$\times\left[\left(\pi T_K\right)^2 + \left(\tilde{\varepsilon}_i - \lambda_K^{(\alpha)}\right)^2\right]\left[1+\exp\left(\frac{\lambda_K^{(\alpha)} - \tilde{\varepsilon}_i}{T_K}\right)\right]^{-1}, \quad \text{(A.1)}$$

K=Fragment1 and Fragment2

α=protons and neutrons

$$T_K(t) = 3.46\sqrt{\frac{E_K^*(t)}{\langle A_K(t)\rangle}} \quad \text{(A.2)}$$

Chemical potential $\lambda_K{}^{(a)}$

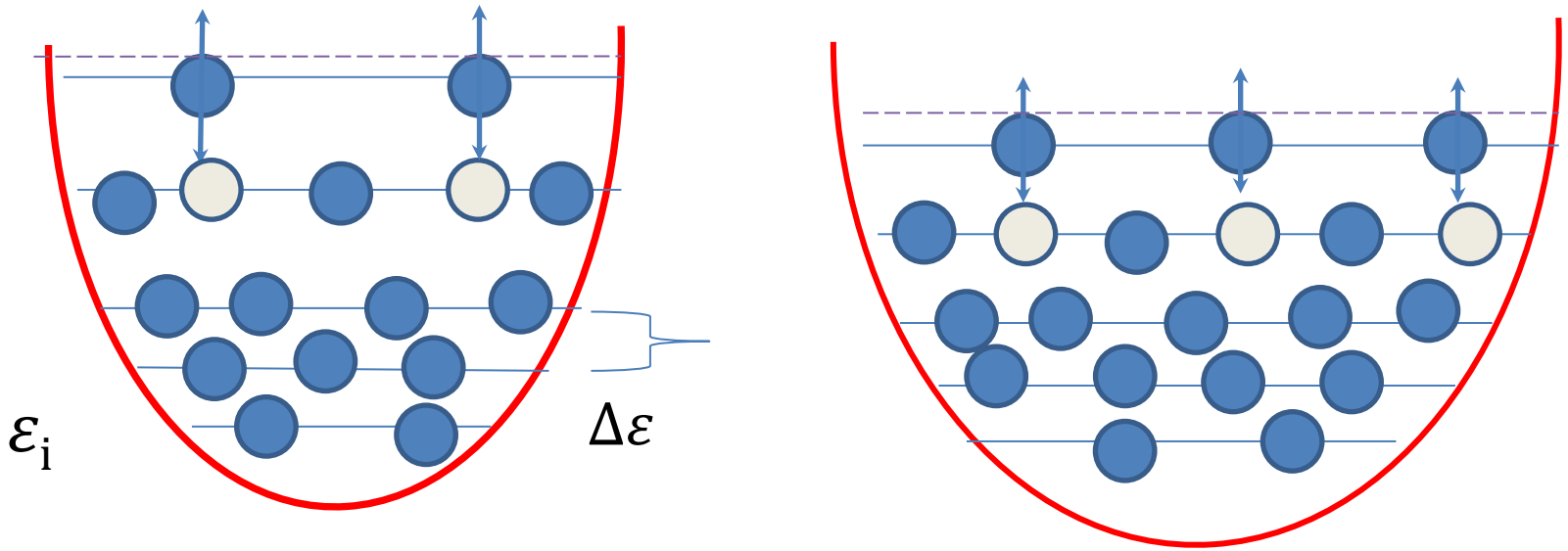

Parameters of the nucleon-nucleon effective forces

A.B.Migdal, Theory of the Finite Fermi—Systems and Properties of Atomic Nuclei, Moscow, Nauka, 1983.

$$\varepsilon_{F_K}^{(Z)} = \varepsilon_F \left[1 - \frac{2}{3}(1 + 2f'_K) \frac{\langle N_K \rangle - \langle Z_K \rangle}{\langle A_K \rangle} \right],$$
$$\varepsilon_{F_K}^{(N)} = \varepsilon_F \left[1 + \frac{2}{3}(1 + 2f'_K) \frac{\langle N_K \rangle - \langle Z_K \rangle}{\langle A_K \rangle} \right], \qquad \text{(A.14)}$$

where $\varepsilon_F = 37$ MeV,

$$f_K = f_{\text{in}} - \frac{2}{\langle A_K \rangle^{1/3}}(f_{\text{in}} - f_{\text{ex}}),$$
$$f'_K = f'_{\text{in}} - \frac{2}{\langle A_K \rangle^{1/3}}(f'_{\text{in}} - f'_{\text{ex}}) \qquad \text{(A.15)}$$

and $f_{\text{in}} = 0.09$, $f'_{\text{in}} = 0.42$, $f_{\text{ex}} = -2.59$, $f'_{\text{ex}} = 0.54$, $g = 0.7$ are the constants of the effective nucleon–nucleon interaction.

Results of calculation of the widths Γ_i of single-particle states of neutrons in the interacting nuclei for the ^{40}Ca+^{248}Cm and ^{48}Ca+^{248}Cm reactions

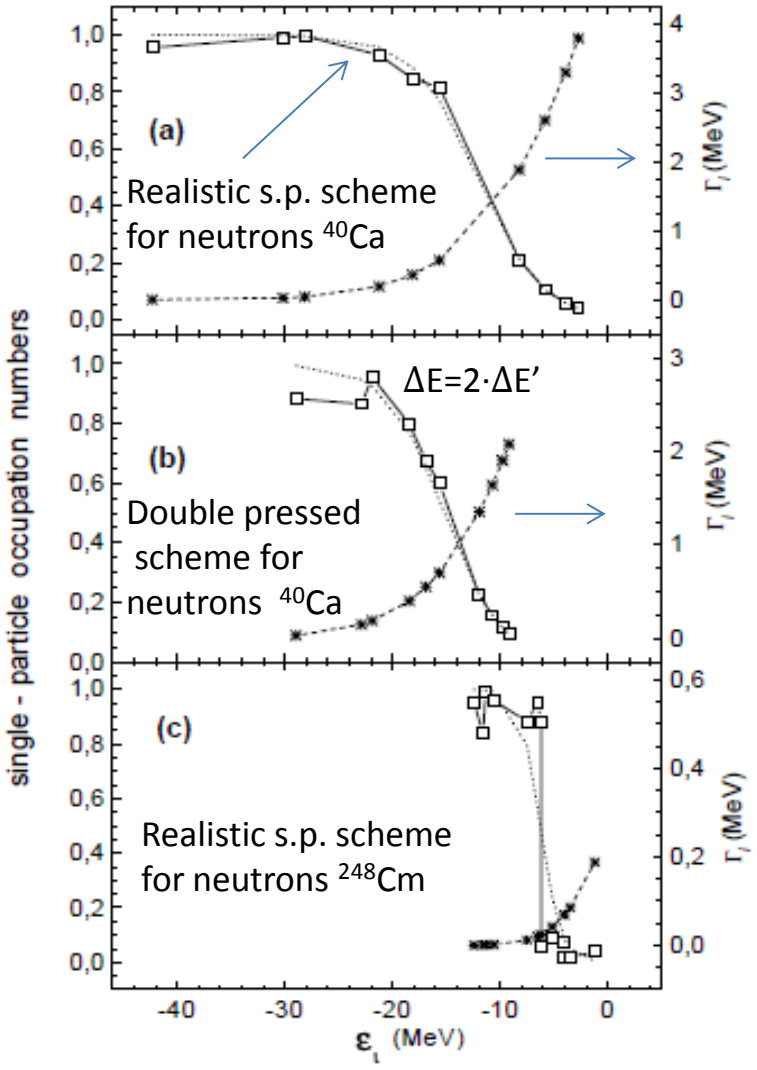

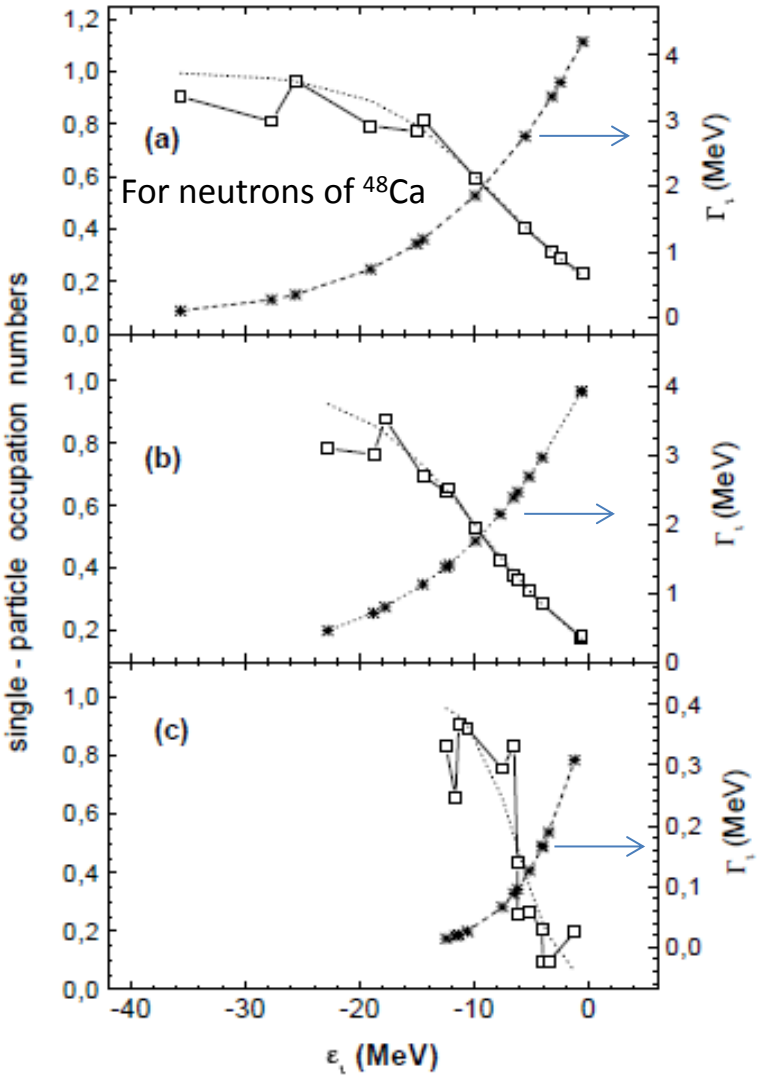

Results of calculation of the widths Γ_i of single-particle states of the protons in the interacting nuclei for the $^{40}Ca+^{248}Cm$ and $^{48}Ca+^{248}Cm$ reactions

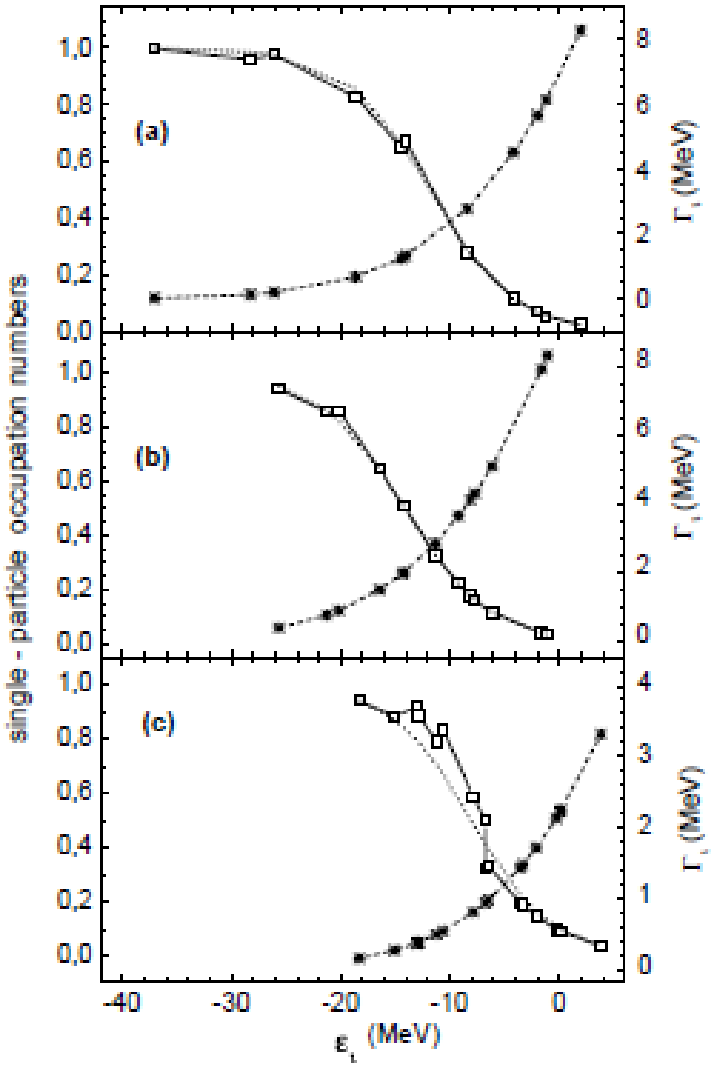

Fig. 5. The same as in fig. 3, but for the proton subsystem in the $^{48}Ca + ^{248}Cm$ reaction.

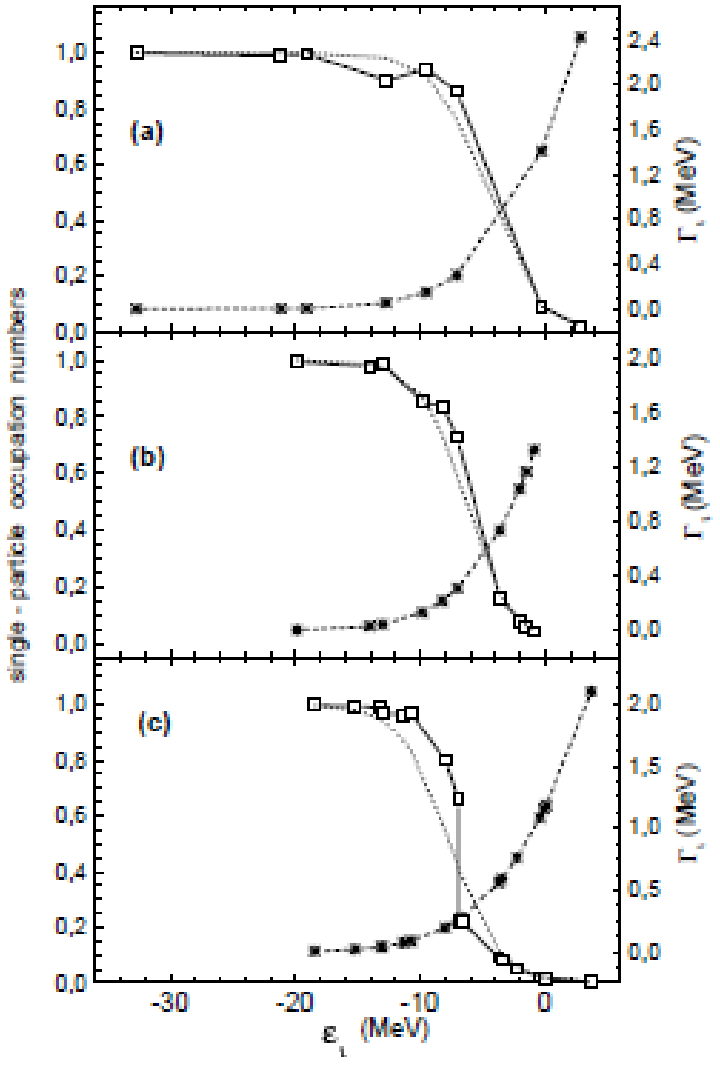

Fig. 6. The same as in fig. 3, but for the proton subsystem in the $^{40}Ca+^{248}Cm$ reaction.

Relaxation times of the single-particle excitations

The relaxation times of the single-particle levels τ_i used in the calculations of an evolution of the single-particle occupation numbers are calculated according to formula (A.1). Near the Fermi surface τ_i changes from $1.7 \cdot 10^{-22}$ s to $6.5 \cdot 10^{-19}$ s. The equilibration time for a Fermi-gas was estimated by Bertsch [20]

$$\tau = 2 \cdot 10^{-22} \mathrm{s\,MeV}/\epsilon^*(t), \qquad (35)$$

where $\epsilon^*(t)$ is the total excitation energy per nucleon. For the reactions under consideration τ is near 10^{-21} which is comparable with the values of τ_i obtained for levels near the Fermi surface.

This relaxation time is considered as transition time between diabatic and adiabatic pPictures of the processes

Friction coefficient is a function of the relaxation time.

Expressions for the friction coefficients

$$\gamma_R(R(t)) = \sum_{i,i'} \left| \frac{\partial V_{ii'}(R(t))}{\partial R} \right|^2 B^{(1)}_{ii'}(t), \qquad \text{(B.1)}$$

$$\gamma_\theta(R(t)) = \frac{1}{R^2} \sum_{i,i'} \left| \frac{\partial V_{ii'}(R(t))}{\partial \theta} \right|^2 B^{(1)}_{ii'}(t), \qquad \text{(B.2)}$$

and the dynamic contribution to the nucleus-nucleus potential

$$\delta V(R(t)) = \sum_{i,i'} \left| \frac{\partial V_{ii'}(R(t))}{\partial R} \right|^2 B^{(0)}_{ii'}(t), \qquad \text{(B.3)}$$

were obtained in [14] by estimation of the evolution of the coupling term between the relative motion of nuclei and the nucleon motion inside nuclei; $B^{(0)}_{ii'}(t)$ and $B^{(1)}_{ii'}(t)$ are calculated as follows:

$$B^{(n)}_{ik}(t) = \frac{2}{\hbar} \int_0^t \mathrm{d}t' (t-t')^n \exp\left(\frac{t'-t}{\tau_{ik}}\right) \times \sin\left[\omega_{ik}\left(\mathbf{R}(t')\right)(t-t')\right] \left[\tilde{n}_k(t') - \tilde{n}_i(t')\right], \qquad \text{(B.4)}$$

$$\hbar\omega_{ik} = \epsilon_i + \Lambda_{ii} - \epsilon_k - \Lambda_{kk}\,. \qquad \text{(B.5)}$$

Mass distribution of the fission products as a function of the excitation energy of compound nucleus

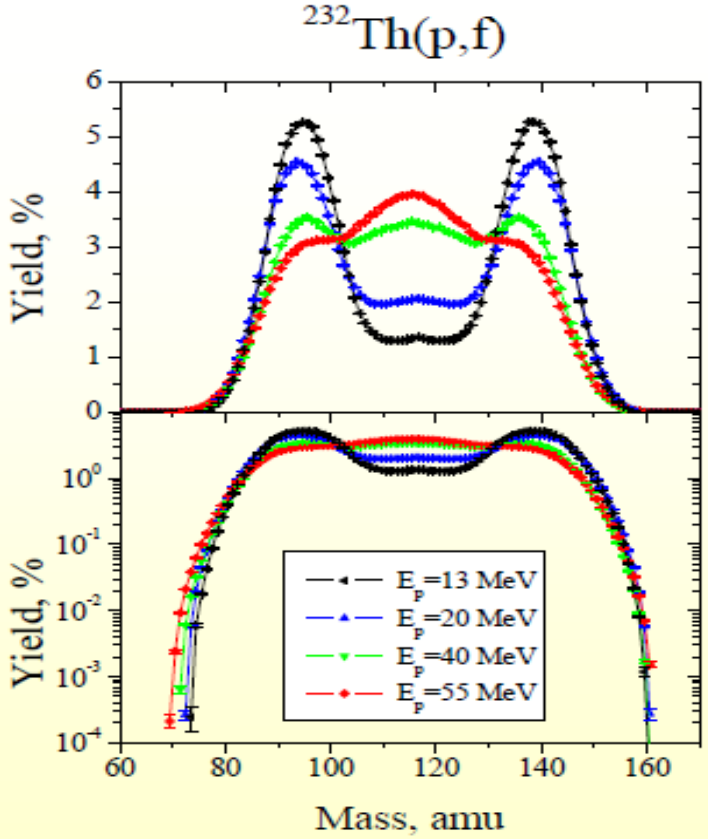

The mass distribution in linear and logarithmic scale for the proton-induced fission of ^{232}Th at the proton energies 13, 20, 40 and 55 MeV

Width of the single-particle excited states

A. Nasirov et al, Nucl. Phys. A 759 (2005) 342–369

$$\Gamma_i = \frac{\hbar}{\tau_i} = \frac{\sqrt{2}\pi}{32\hbar\varepsilon_{F_K}^{(\alpha)}}\left[(f_K - g)^2 + \frac{1}{2}(f_K + g)^2\right]$$

$$\times\left[\left(\pi T_K\right)^2 + \left(\tilde{\varepsilon}_i - \lambda_K^{(\alpha)}\right)^2\right]\left[1 + \exp\left(\frac{\lambda_K^{(\alpha)} - \tilde{\varepsilon}_i}{T_K}\right)\right]^{-1}, \quad \text{(A.1)}$$

where

$$T_K(t) = 3.46\sqrt{\frac{E_K^*(t)}{\langle A_K(t)\rangle}} \quad \text{(A.2)}$$

E_K is A_K excitation energy and mass number of the fragment *K*

D. Pines, P. Noziéres, Theory of Quantum Liquids, Benjamin, New York, 1966

Emission of neutrons does not change strongly the kinetic energy distribution of the fission fragments.

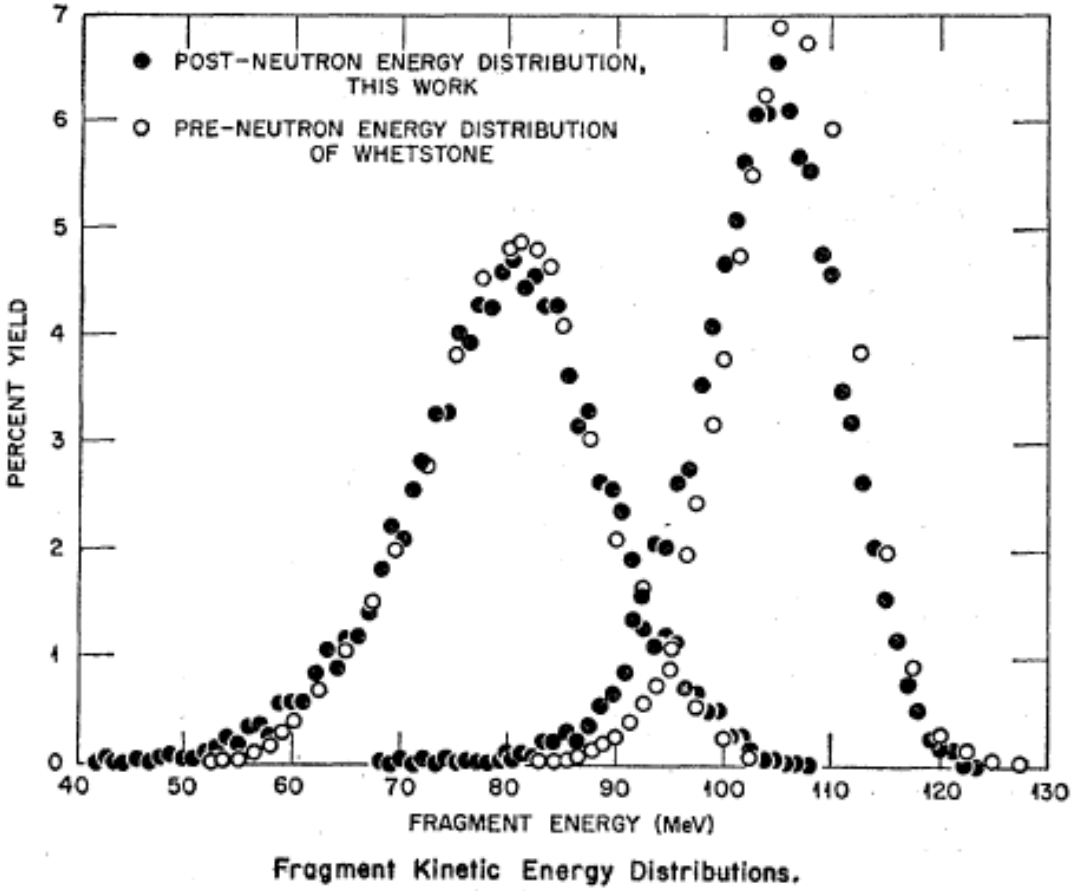

FIG. 5. Post-neutron-emission kinetic energy distributions for the light and heavy fragments from ^{252}Cf fission, compared with the pre-neutron-emission distributions of Whetstone (Ref. 4).

Note,

3) Due to the shell structure of being formed fragments the share of the excitation energy released from the binding energy of the compound nucleus is no equilibrated:

$T_1 \neq T_2$, i.e. excitation energies of both fragments are not distributed proportionally to their masses

$$\frac{E_1}{A_1} \neq \frac{E_2}{A_2}$$

This is seen from the neutron multiplicity – number of the emitted neutrons from the each fission fragments.

Yield neutrons and gamma quanta in coincidence with the fission fragments

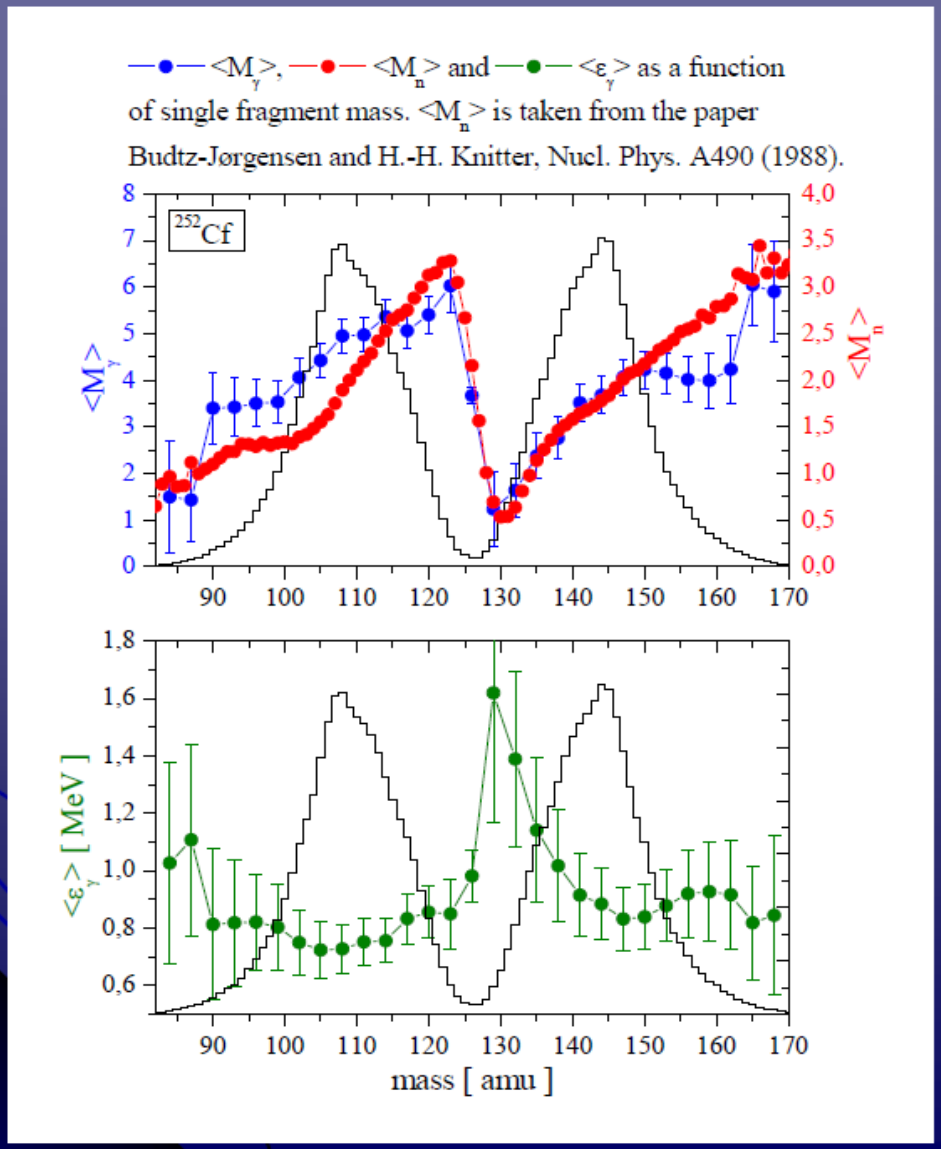

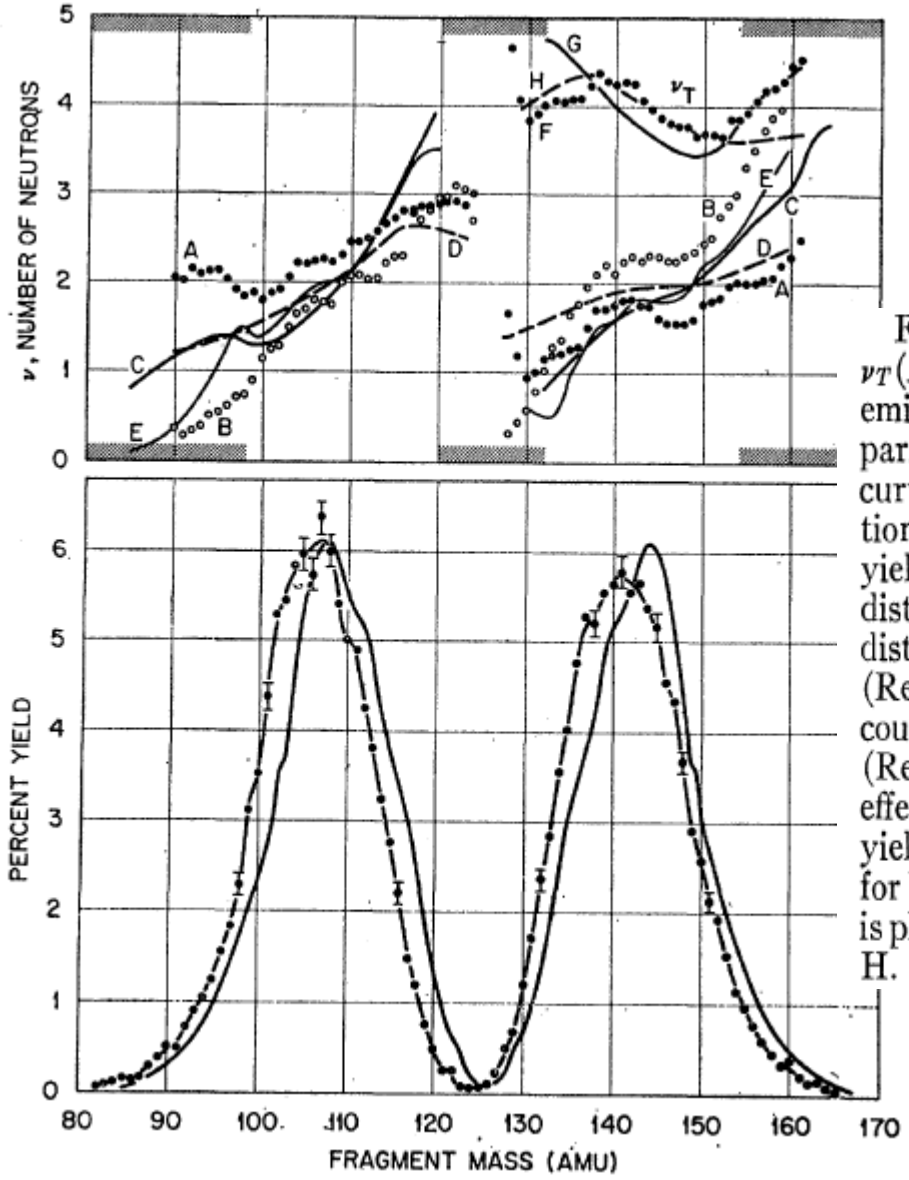

FIG. 8. Mass distributions and number of neutrons $\nu(M^*)$, and $\nu_T(M^*)$. In the lower part of the figure the present post-neutron-emission mass distribution is shown (points and curve) in comparison with the pre-neutron-emission mass distribution (smooth curve) of Whetstone (Ref. 4). Neither curve is corrected for resolution. The upper part of the figure shows $\nu(M^*)$ from cumulative yield calculations in which the present, resolution-corrected mass distribution was used in combination with the resolution-corrected distributions of Whetstone (Ref. 4), curve A, and of Fraser *et al.* (Ref. 5), curve B. Curves C and D show the results of neutron counting experiments of Bowman *et al.* (Ref. 7) and Whetstone (Ref. 19), respectively. Curve D is not corrected for resolution effects. Curve E shows the results of Terrell's earlier cumulative yield calculations (Ref. 18). The total number of neutrons ν_T for both fragments, obtained respectively from curves A, C, and D, is plotted as a function of heavy fragment mass in curves F, G, and H. See text.

G.G. Adamian, R.V. Jolos, A.K. Nasirov, "Partition of excitation energy between reaction products in heavy ion collisions", ZEITSCHRIFT FOR PHYSIK A 347, 203-210 (1994)

The role of the particle-hole excitations and the nucleon exchange is considered. The ratio of the projectile excitation energy to the total excitation energy for the reactions ^{238}U(1468 MeV)+^{124}Sn, ^{238}U(1398 MeV)+^{124}Sn ^{56}Fe(505 MeV)+ ^{165}Ho, ^{74}Ge (629 MeV)+ ^{165}Ho and ^{68}Ni(880 MeV)+ ^{197}Au is calculated. The results of calculations are in good agreement with the experimental data.

The total Hamiltonian of a dinuclear system $\hat{H}$ takes the form

$$\hat{H} = \hat{H}_{\text{rel}} + \hat{H}_{\text{in}} + \hat{V}_{\text{int}} \tag{1}$$

The Hamiltonian of a relative motion

$$\hat{H}_{\text{rel}} = \frac{\hat{\mathbf{P}}^2}{2\mu} + \hat{U}(\hat{\mathbf{R}})$$

consists of the kinetic energy and nucleus-nucleus interaction potential $\hat{U}(\hat{\mathbf{R}})$. Here $\hat{\mathbf{R}}$ is relative distance between the center of the mass of fragments, $\hat{\mathbf{P}}$ is a conjugate momentum, μ is a reduced mass of the system. The last two terms in (1) describe the intrinsic motion of nuclei and the coupling between relative and intrinsic motion. By means of the Ehrenfest theorem, it is easy to obtain from (1) the classical limit of equations of motion for the macroscopical collective variables $\mathbf{R}$ and $\mathbf{P}$:

$$\dot{\mathbf{R}} = \nabla_P (H_{\text{rel}} + \langle t | \hat{V}_{\text{int}} | t \rangle), \tag{2}$$

$$\dot{\mathbf{P}} = -\nabla_R (H_{\text{rel}} + \langle t | \hat{V}_{\text{int}} | t \rangle), \tag{3}$$

The single-particle basis is constructed from the asymptotic single-particle state vectors of noninteracting nuclei: for projectile "P"$|P\rangle$ and target "T"$|T\rangle$ in the form

$$|\tilde{P}\rangle = |P\rangle - \tfrac{1}{2}\sum_{T} |T\rangle\langle T|P\rangle,$$

$$|\tilde{T}\rangle = |T\rangle - \tfrac{1}{2}\sum_{P} |P\rangle\langle P|T\rangle.$$

The orthogonality condition for the given basis is fulfilled up to the second order of the overlapping integral $\langle P|T\rangle$ [30].

There are two interacting nuclei – projectile and target which have Z_P and Z_T protons, and N_P and N_T neutrons, respectively. The protons and neutrons are placed on the corresponding single-particle states created by the mean-fields U_P and U_T.
The quantum numbers and energies of these single-particle states are found by solving the Schrödinger equation with the Hamiltonians for both nuclei

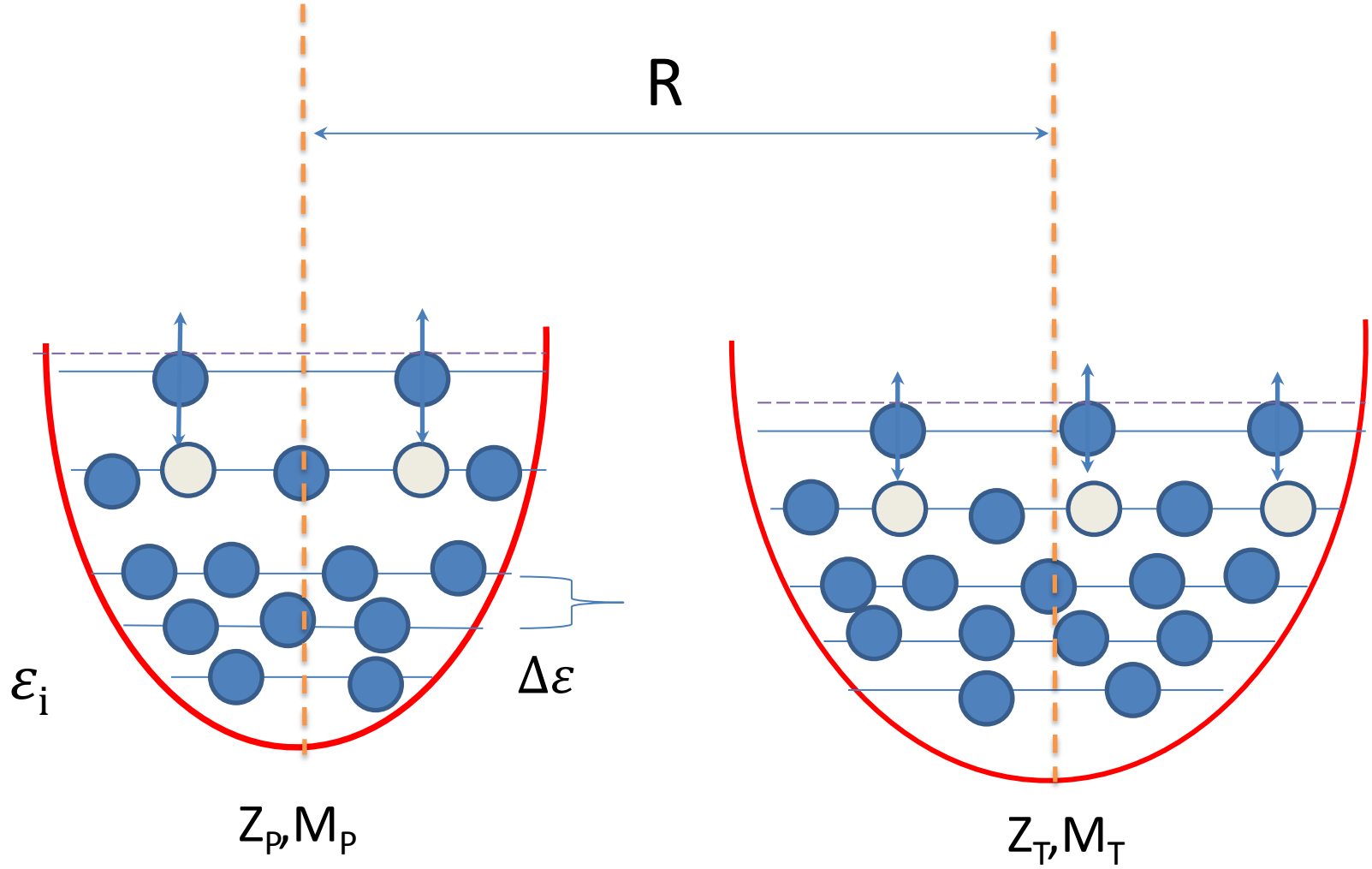

The single-particle Hamiltonian of a dinuclear system $\hat{\mathscr{H}}$ is as follows

$$H_{\text{in}}\big(R(t)\big) = \sum_{i=1}^{A}\left(\frac{-\hbar^2}{2m}\Delta_i + \hat{U}_P(\mathbf{r}_i - \mathbf{R}(t)) + \hat{U}_T(\mathbf{r}_i)\right), \tag{4}$$

where m is the nucleon mass, and $A = A_P + A_T$ is the total number of nucleons in the system. The average single-particle potentials of projectile U_P and target U_T include both the nuclear and the Coulomb fields.

Hamiltonian of the interacting nuclei of the dinuclear system

In the second quantization form the Hamiltonian (4) can be rewritten as

$$\hat{\mathscr{H}}(\mathbf{R}(t)) = \hat{H}_{\rm in}(\mathbf{R}(t)) + \hat{V}_{\rm int}(\mathbf{R}(t)),$$

$$\hat{H}_{\rm in}(\mathbf{R}(t)) = \sum_i \tilde{\varepsilon}_i(\mathbf{R}(t))\, a_i^+ a_i = \sum_P \tilde{\varepsilon}_P(\mathbf{R}(t))\, a_P^+ a_P + \sum_T \tilde{\varepsilon}_T(\mathbf{R}(t))\, a_T^+ a_T, \tag{5}$$

$$\hat{V}_{\rm int}(\mathbf{R}(t)) = \sum_{i \neq i'} V_{ii'}(\mathbf{R}(t))\, a_i^+ a_{i'} = \sum_{P \neq P'} \chi_{PP'}^{(T)}(\mathbf{R}(t))\, a_P^+ a_{P'} + \sum_{T \neq T'} \chi_{TT'}^{(P)}(\mathbf{R}(t))\, a_T^+ a_{T'} + \sum_{T,P} g_{PT}(\mathbf{R}(t))(a_P^+ a_T + \text{h.c.}).$$

Taking into account the influence of the partner nucleus mean-field on single-particle states.

In the expression (6) $\varepsilon_{P(T)}$ are single-particle energies of nonperturbed states in the projectile (target) nucleus. These states are characterized by the set of quantum numbers $P \equiv (n_P, j_P, l_P, m_P)$ and $T \equiv (n_T, j_T, l_T, m_T)$. The diagonal matrix elements $\langle P|U_T|P\rangle$ and $\langle T|U_P|T\rangle$ determine the shifts of the single-particle energies of the projectile nucleus caused by the target mean field. The corresponding nondiagonal matrix elements $\chi^{(T)}_{P'P}$ and $\chi^{(P)}_{T'T}$ generate particle-hole transitions in the same nucleus. The matrix elements g_{PT} correspond to the nucleon exchange between the reaction partners owing to the nonstationary mean field of a dinuclear system. The contribution of noninertial recoil effects to the matrix elements are neglected since they are small [21].

21. Boose, D., Richert, J.: Nucl. Phys. A **433**, 511 (1985)

Taking into account the influence of the partner nucleus mean-field on single-particle states.

The effect of the presence of the partner – nucleus on the single-particle states of considered nucleus is taken into account by the perturbation theory:

Up to the second order in $\langle P | T \rangle$

$$
\begin{aligned}
\tilde{\varepsilon}_P(\mathbf{R}(t)) &= \varepsilon_P + \langle P | U_T(\mathbf{r}) | P \rangle, \\
\tilde{\varepsilon}_T(\mathbf{R}(t)) &= \varepsilon_T + \langle T | U_P(\mathbf{r} - \mathbf{R}(t)) | T \rangle, \\
\chi^{(T)}_{PP'}(\mathbf{R}(t)) &= \langle P | U_T(\mathbf{r}) | P' \rangle, \\
\chi^{(P)}_{TT'}(\mathbf{R}(t)) &= \langle T | U_P(\mathbf{r} - \mathbf{R}(t)) | T' \rangle, \\
g_{PT}(\mathbf{R}(t)) &= \tfrac{1}{2} \langle P | U_P(\mathbf{r} - \mathbf{R}(t)) + U_T(\mathbf{r}) | T \rangle.
\end{aligned}
\qquad (6)
$$

Calculations of the single-particle density matrix elements

The equation of motion for the single-particle density-matrix $\hat{n}(t)$ is

$$i\hbar \frac{\partial \hat{n}(t)}{\partial t} = [\hat{\mathscr{H}}(\mathbf{R}(t)), \hat{n}(t)] . \tag{7}$$

In the matrix representation it takes the form

$$i\hbar \frac{\mathrm{d}\, n_i(t)}{\mathrm{d}\, t} = \sum_k [V_{ik}(\mathbf{R}(t))\, n_{ki}(t) - n_{ik}(t)\, V_{ki}(\mathbf{R}(t))], \tag{8}$$

$$i\hbar \frac{\mathrm{d} n_{ik}(t)}{\mathrm{d}\, t} = \hbar\, \tilde{\omega}_{ik}(\mathbf{R}(t))\, n_{ik}(t) + V_{ki}(\mathbf{R}(t))[n_k(t) - n_i(t)], \tag{9}$$

where the following notations $\tilde{\omega}_{ik}(\mathbf{R}(t)) = [\tilde{\varepsilon}_i(\mathbf{R}(t)) - \tilde{\varepsilon}_k(\mathbf{R}(t))]/\hbar$, $n_{ik}(t) = \langle t | a_i^+ a_k | t \rangle$, $n_i(t) = n_{ii}(t)$

$$\sum_{k'} V_{k'i}(\mathbf{R}(t))\, n_{k'k}(t) - \sum_{i'} V_{ki'}(\mathbf{R}(t))\, n_{ii'}(t) \approx V_{ki}(\mathbf{R}(t))[n_k(t) - n_i(t)] . \tag{10}$$

Calculations of the transition matrix elements

$$g_{pT}(R)=\int_{\infty} d^3\mathbf{r}\,\varphi_T^*(\mathbf{r})\left[\frac{1}{2}(U_T(\mathbf{r})+U_p(\mathbf{r}-\mathbf{R}))\right]\varphi_p(\mathbf{r}-\mathbf{R}),$$

As a wave functions $\varphi_P{}^*$ and $\varphi_T{}^*$ we used the solutions of the Schrödinger equation with the symmetrical rectangle potential well with the given depth U_P and U_T, respectively. The single-particle energies were found as own values of the Wood-Saxon potential which is more realistic for the atomic nuclei.

Up to the second order in $\langle P|T\rangle$

$$\begin{aligned}
\tilde{\varepsilon}_P(\mathbf{R}(t)) &= \varepsilon_P+\langle P|U_T(\mathbf{r})|P\rangle,\\
\tilde{\varepsilon}_T(\mathbf{R}(t)) &= \varepsilon_T+\langle T|U_P(\mathbf{r}-\mathbf{R}(t))|T\rangle,\\
\chi^{(T)}_{PP'}(\mathbf{R}(t)) &= \langle P|U_T(\mathbf{r})|P'\rangle, \qquad (6)\\
\chi^{(P)}_{TT'}(\mathbf{R}(t)) &= \langle T|U_P(\mathbf{r}-\mathbf{R}(t))|T'\rangle,\\
g_{PT}(\mathbf{R}(t)) &= \tfrac{1}{2}\langle P|U_P(\mathbf{r}-\mathbf{R}(t))+U_T(\mathbf{r})|T\rangle.
\end{aligned}$$

Calculations of the single-particle density matrix elements

$$n_{ik}(t)=\frac{1}{i\hbar}\int_{t_0}^{t} \mathrm{d}\,t'\; V_{ik}(\mathbf{R}(t'))$$

$$\cdot\exp\left\{i\int_{t'}^{t}\mathrm{d}\,t''\;\tilde{\omega}_{ki}(\mathbf{R}(t''))\right\}\;[n_k(t')-n_i(t')] \qquad (11)$$

into (8), we obtain equations for the dynamical occupation numbers $n_i(t)$

$$\frac{\mathrm{d}\,n_i(t)}{\mathrm{d}\,t}=\sum_k\int_{t_0}^{t}\mathrm{d}\,t'\;\Omega_{ik}(t,t')[n_k(t')-n_i(t')] \qquad (12)$$

where

$$\Omega_{ik}(t,t')=\frac{2}{\hbar^2}\,\mathrm{Re}\left\{V_{ik}(\mathbf{R}(t))\;V_{ki}(\mathbf{R}(t'))\right.$$

$$\left.\cdot\exp\left[i\int_{t'}^{t}\mathrm{d}\,t''\;\tilde{\omega}_{ki}(\mathbf{R}(t''))\right]\right\}.$$

Calculations of the single-particle density matrix elements

Equation (12) contains memory effects. In Markovian approximation Eq. (12) can be rewritten in a master-equation form

$$\frac{\mathrm{d}\, n_i(t)}{\mathrm{d}\, t} = \sum_k w_{ik}(t, t_0)\left[n_k(t) - n_i(t)\right], \tag{13}$$

where

$$w_{ik}(t, t_0) = \int_{t_0}^{t} \mathrm{d}\, t'\ \Omega_{ik}(t, t').$$

$$\Omega_{ik}(t, t') = \frac{2}{\hbar^2}\,\mathrm{Re}\left\{V_{ik}(\mathbf{R}(t))\, V_{ki}(\mathbf{R}(t')) \cdot \exp\left[i \int_{t'}^{t} \mathrm{d}\, t''\ \tilde{\omega}_{ki}(\mathbf{R}(t''))\right]\right\}.$$

$$g_{p\tau}(R) = \int_{\infty} d^3\mathbf{r}\ \varphi_\tau^*(\mathbf{r})\left[\frac{1}{2}\left(U_\tau(\mathbf{r}) + U_p(\mathbf{r}-\mathbf{R})\right)\right]\varphi_p(\mathbf{r}-\mathbf{R}),$$

Solution of the master equation for the nucleon transfer

Equation (13) can be solved by the successive iteration procedure

$$n_i(t+\Delta t)=n_i(t)+\sum_k \bar{W}_{ik}(\mathbf{R}(t),\Delta t)[n_k(t)-n_i(t)],$$

$$\bar{W}_{ik}(\mathbf{R}(t),\Delta t)=|V_{ik}(\mathbf{R}(t))|^2 \frac{\sin^2\left(\frac{\Delta t}{2}\tilde{\omega}_{ki}(\mathbf{R}(t))\right)}{\left[\frac{\hbar}{2}\tilde{\omega}_{ki}(\mathbf{R}(t))\right]^2}. \qquad (14)$$

The initial values of the occupation numbers are equal to 1 for occupied states and zero for the unoccupied one. A magnitude of the time step Δt used in the calculations is $(0.3 \div 0.7)\cdot 10^{-22}$ s.

Irreversibility of the solution of master equation

$$\frac{\mathrm{d}\, n_i(t)}{\mathrm{d}\, t} = \sum_k w_{ik}(t,\, t_0)\left[n_k(t) - n_i(t)\right],$$

for the occupation numbers can be proved by calculating the derivative of the entropy of system:

$$\frac{\mathrm{d}\, S(t)}{\mathrm{d}\, t} = \frac{k}{2} \sum_{i,k} w_{ik}(\mathbf{R}(t),\, \Delta t)\left[n_i(t)\, \bar{n}_k(t) - n_k(t)\, \bar{n}_i(t)\right] \ln\left[\frac{n_i(t)\, \bar{n}_k(t)}{\bar{n}_i(t)\, n_k(t)}\right]$$

$$\bar{n}_i = 1 - n_i$$

where k is the Boltzmann constant. It is seen that the entropy derivative is larger than or equal to zero. This irreversibility is a consequence of the assumption of the non-diagonal matrix

$$\sum_{k'} V_{k'i}(\mathbf{R}(t))\, n_{k'k}(t) - \sum_{i'} V_{ki'}(\mathbf{R}(t))\, n_{ii'}(t) \approx V_{ki}(\mathbf{R}(t))\left[n_k(t) - n_i(t)\right]. \qquad (10)$$

Including the residual forces in the master equation

The explicit account of the residual interaction requires voluminous calculations. The linearization of the two-body collision integral simplifies the considerations. In the relaxation time approximation [Köhler, H.S.: Nucl. Phys. A343, 315 (1980); ibid 378,181 (1982)] our master equation has the next operator shape:

$$i\hbar \frac{\partial \hat{\tilde{n}}(t)}{\partial t} = [\hat{\mathscr{H}}, \hat{\tilde{n}}(t)] - \frac{i\hbar}{\tau} [\hat{\tilde{n}}(t) - \hat{\tilde{n}}^{eq}(\mathbf{R}(t))],$$

where τ is the relaxation time, and $\hat{\tilde{n}}^{eq}(R(t))$ is a local quasi-equilibrium density matrix at fixed value of the collective coordinate $R(t)$, which is determined by the excitation energy of each nucleus.

$$< \hat{\tilde{n}}^{eq}\left(R(t)\right) >= 1/\left[1 + \exp\left(\frac{\varepsilon - \lambda}{T}\right)\right]$$

where ε and λ are single-particle energy of nucleons and T is the effective temperature.

Master equations for the density matrix in the tau-approximation method

$$i\hbar \frac{\mathrm{d}\tilde{n}_i(t)}{\mathrm{d}t} = \sum_k \left[V_{ik}(\mathbf{R}(t))\,\tilde{n}_{ki}(t) - V_{ki}(\mathbf{R}(t))\,\tilde{n}_{ik}(t)\right]$$

$$- \frac{i\hbar}{\tau}\left[\tilde{n}_i(t) - \tilde{n}_i^{\mathrm{eq}}(\mathbf{R}(t))\right], \qquad (8')$$

$$i\hbar \frac{\mathrm{d}\tilde{n}_{ik}(t)}{\mathrm{d}t} = \hbar\left[\tilde{\omega}_{ik}(\mathbf{R}(t)) - \frac{i}{\tau}\right]\tilde{n}_{ik}(t) + V_{ki}(\mathbf{R}(t))\left[\tilde{n}_k(t) - \tilde{n}_i(t)\right], \qquad (9')$$

which are solved only numerically at known matrix elements V_{ik}

Solutions for the density matrixes

$$\tilde{n}_i(t) = \exp\left(\frac{t_0 - t}{\tau}\right)\left\{\tilde{n}_i(t_0) + \sum_k \int_{t_0}^{t} \mathrm{d}\,t' \int_{t_0}^{t'} \mathrm{d}\,t''\ \Omega_{ik}(t', t'')\right.$$

$$\cdot \exp\left(\frac{t'' - t}{\tau}\right)\left[\tilde{n}_k(t'') - \tilde{n}_i(t'')\right]$$

$$\left. + \int_{t_0}^{t} \mathrm{d}\,t'\ \tilde{n}_i^{\mathrm{eq}}(\mathbf{R}(t')) \exp\left(\frac{t' - t_0}{\tau}\right)\right\}. \qquad (17)$$

$$\tilde{n}_{ik}(t) = \frac{1}{i\hbar} \int_{t_0}^{t} \mathrm{d}\,t'\ V_{ik}(\mathbf{R}(t'))$$

$$\cdot \exp\left\{i \int_{t'}^{t} \mathrm{d}\,t'' \left[\tilde{\omega}_{ki}(\mathbf{R}(t'')) + \frac{i}{\tau}\right]\right\}\left[\tilde{n}_k(t') - \tilde{n}_i(t')\right],$$

where $$\Omega_{ik}(t, t') = \frac{2}{\hbar^2}\,\mathrm{Re}\left\{V_{ik}(\mathbf{R}(t))\ V_{ki}(\mathbf{R}(t'))\right.$$

$$\left. \cdot \exp\left[i \int_{t'}^{t} \mathrm{d}\,t''\ \tilde{\omega}_{ki}(\mathbf{R}(t''))\right]\right\}.$$

and $\hat{\omega}_{ki} = (\hat{\varepsilon}_k - \hat{\varepsilon}_i)/\hbar$

Time evolution of the occupation numbers of protons and neutrons in interacting nuclei.

It is convenient to solve (17) step by step, dividing time interval $(t-t_0)$ into parts: t_0, $t_0+\Delta t$, $t_0+2\Delta t$, etc. Then (17) can be rewritten approximately for $\Delta t < \tau$ as

$$\tilde{n}_i(t) = \tilde{n}_i^{eq}(\mathbf{R}(t))\left[1-\exp\left(\frac{-\Delta t}{\tau}\right)\right]+f_i(t)\exp\left(\frac{-\Delta t}{\tau}\right),$$

$$f_i(t) = \tilde{n}_i(t-\Delta t)+\sum_k \bar{W}_{ik}(\mathbf{R}(t),\Delta t)$$

$$\cdot\left[\tilde{n}_k(t-\Delta t)-\tilde{n}_i(t-\Delta t)\right], \qquad (18)$$

Non-equilibrium processes in heavy ion collisions

At $A_1 + A_2 \rightarrow A_1' + A_2'$ usually $E_1^* : E_2^* \neq A_1' : A_2'$ (even at fission!).
At thermodynamic equilibrium must be $T_1 = T_2 \rightarrow E_1^* : E_2^* = A_1' : A_2'$

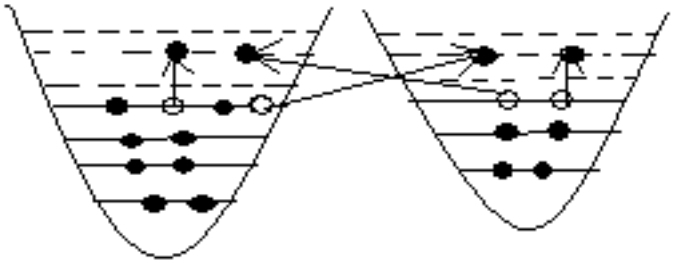

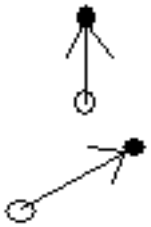

$$T_i = 3.46\sqrt{E_i^* / A_i}$$

i=P,T

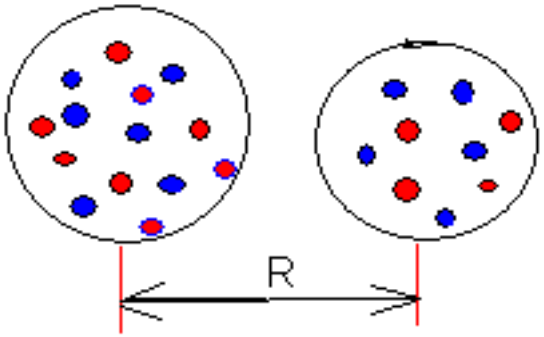

$$E_P^* = E_P^{*(ph)} + E_P^{*(ex)}$$

R.V. Jolos, Eur. Phys. Jour. A**7**, 2000, p.115-224

Calculation of the physical quantities characterizing multinucleon transfer reactions

The present model allows us to calculate the average number of protons $\langle Z_{P(T)} \rangle$ or neutrons $\langle N_{P(T)} \rangle$ and their variance σ_Z^2 or σ_N^2, and to determine the intrinsic excitation energies $E^*_{P,T}(t)$ for every nucleus:

$$\langle Z_{P(T)} \rangle(t) = \sum_{P(T)}^{Z} \tilde{n}_{P(T)}(t), \tag{19}$$

$$\langle N_{P(T)} \rangle(t) = \sum_{P(T)}^{N} \tilde{n}_{P(T)}(t), \tag{20}$$

$$\sigma^2_{Z(N)}(t) = \sum_{P}^{Z(N)} \tilde{n}_P(t)[1 - \tilde{n}_P(t)], \tag{21}$$

$$E^*_{P(T)}(t + \Delta t) = E^*_{P(T)}(t) + \sum_{P(T)} [\tilde{\varepsilon}_{P(T)}(\mathbf{R}(t)) - \varepsilon_{F_{P(F_T)}}(\mathbf{R}(t))] \cdot [\tilde{n}_{P(T)}(t + \Delta t) - \tilde{n}_{P(T)}(t)], \tag{22}$$

where $\varepsilon_{F_{P(F_T)}}(\mathbf{R}(t))$ is the Fermi energy of a projectile-like nucleus "P" or target-like nucleus "T". The top index

Calculation of the excitation energy of nucleus

One of our aims is to calculate the ratio of the excitation energies of the projectile-like (E_P^*) and target-like (E_T^*) fragments

$$R_{P/T} = E_P^*/E_T^*. \tag{25}$$

We defined a change of the excitation energy of the proton (P) (or neutron (N)) subsystem in each of the colliding nuclei by the following equation

$$\begin{aligned} E_P^*(t+\Delta t) = E_P^*(t) &+ \langle \hat{\mathcal{H}}_P(\mathbf{R},\xi) - \lambda_P \hat{N}_P \rangle_{t+\Delta t} \\ &- \langle \hat{\mathcal{H}}_P(\mathbf{R},\xi) - \lambda_P \hat{N}_P \rangle_t \,. \end{aligned} \tag{26}$$

where H_P, λ_P and N_P are Hamiltonian, chemical potential and number nucleons, respectively, for the projectile-like nuclei.

Calculation of the excitation energy of nucleus

Using explicit expressions for $\hat{\mathcal{H}}_P$ and $\hat{N}_P$, as well as performing averaging, we obtain

$$E^*_P(t+\Delta t) = E^*_P(t) + \sum_{i_P} \big[\Delta\varepsilon_{i_P}(t)) - \Delta\lambda_P(t)\big]\tilde{n}_{i_P}(t+\Delta t) + \sum_{i_P} \big[(\tilde{\varepsilon}_{i_P}(t) - \lambda_P(t)\big]\Delta n_{i_P}(t)\,. \qquad (27)$$

Here $\Delta\varepsilon$, Δn and $\Delta\lambda$ are the changes of the single-particle energies, the occupation numbers and the chemical potential, respectively, during time interval Δt.

Our calculations have shown that a contribution of the second term in (27) to the excitation energy is negligibly small, namely $\Delta E^*_P(t)/E^*_P(t) \leq 0.01$.

Calculation of the excitation energy of nucleus

Therefore, the excitation energies of the proton $E^{*(Z)}_{P(T)}$ and neutron $E^{*(N)}_{P(T)}$ subsystems in nuclei are calculated step by step along the time scale using the equation

$$E^*_{P(T)}(t+\Delta t) = E^*_{P(T)}(t) + \sum_{i_P(j_T)} \left[\tilde{\varepsilon}_{i_P(j_T)}(\mathbf{R}(t)) - \lambda_{P(T)}(\mathbf{R}(t))\right] \times \left[\tilde{n}_{i_P(j_T)}(t+\Delta t) - \tilde{n}_{i_P(j_T)}(t)\right]. \quad (28)$$

It should be stressed that the effect of the single-particle energy changes is taken into account in this expression, since at every time step Δt the new values of the renormalized single-particle energies are substituted into the eq. (28) in accordance with the eq. (13).

$$\tilde{\varepsilon}_P(\mathbf{R}) = \varepsilon_P + \langle P|V_T(\mathbf{r})|P\rangle, \quad (13)$$

Total kinetic energy loss

$$E_{\text{loss}} = E_P^* + E_T^*, \tag{29}$$

where $E_P^* = E_P^{*(Z)} + E_P^{*(N)}$ and $E_T^* = E_T^{*(Z)} + E_T^{*(N)}$.

So, our model allows us to calculate excitation energy of the interacting nuclei as a sum of the excitation energy of their proton and neutron subsystems. This is important in case of calculation of the pre-equilibrium emission of protons or neutrons at more high energies relative to the Coulomb barrier of the entrance channel.

Comparison of the calculated results for mean values of the charge and mass numbers in $^{56}Fe+^{165}Ho$ and $^{74}Ge+^{165}Ho$ reactions.

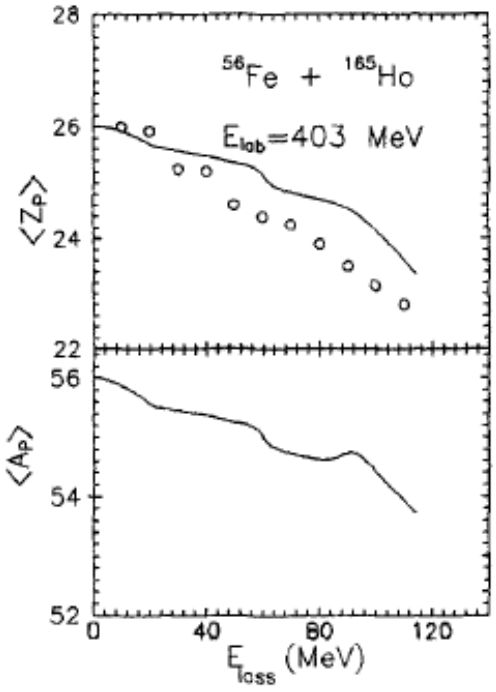

Fig. 8. As Fig. 6, but for the reaction $^{56}Fe(403\ MeV)+^{165}Ho$

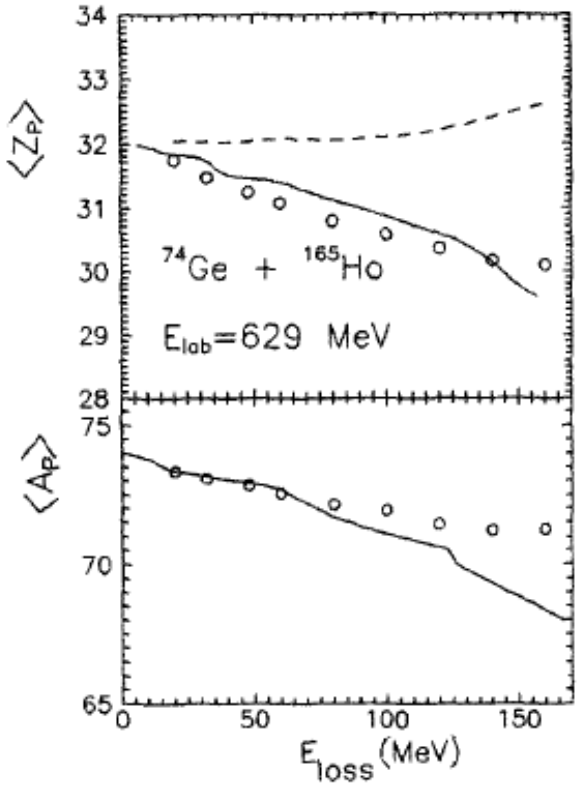

Fig. 10. As Fig. 6, but for the reaction $^{74}Ge(629\ MeV)+^{165}Ho$

Comparison of the ratio of the light fragment excitation energy to the total excitation energy of reaction products.

$$R=\frac{E_P^*}{E_P^*+E_T^*}$$

E_P^* and E_T^* consists from excitation energies of the particle-hole excitations in the interacting nuclei and nucleon exchange process between them:

$$E_P^* = E_P^{*(ph)} + E_P^{*(ex)}$$

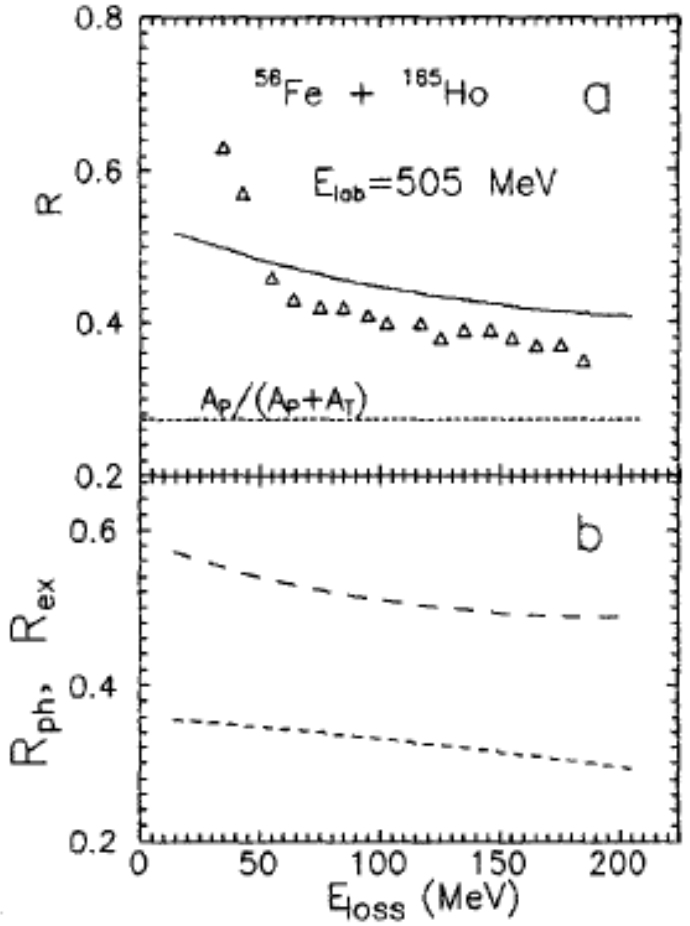

Fig. 1. a Ratio R_P of the projectile-like fragment excitation energy (E_P^*) to the total excitation energy for reaction ^{56}Fe(505 MeV) + ^{165}Ho as a function of the total excitation energy $E_{loss}=E_P^*+E_T^*$. *Triangles* mark the experimental data. *Solid line* presents the theoretical result of our model. *Dotted line* corresponds to thermal equilibrium ($E_P^*/E_{loss}=A_P/(A_P+A_T)$). **b** Calculated ratios $R_P^{(ex)}=E_P^{*(ex)}/(E_P^{*(ex)}+E_T^{*(ex)})$, $R_P^{(ph)}=E_P^{*(ph)}/(E_P^{*(ph)}+E_T^{*(ph)})$ for the reaction ^{56}Fe(505 MeV) + ^{165}Ho as a function of total excitation energy E_{loss} are presented by *long dashed line* and *short dashed line*, respectively

Classification of the nuclear reactions in heavy ion collisions

Early studies of reaction mechanisms between heavy ions have shown that, in a Wilczynski diagram, a definite evolution towards negative scattering angles with increasing energy loss is present, so that the scattering angle was used as an estimate of the interaction time. As usual three regions can be distinguished:

(i) the elastic or quasi-elastic component,

(ii) the partially damped region where the nuclear forces bend the trajectories toward smaller scattering angles and

(iii) the fully relaxed component, where negative angle scattering (or orbiting), fusion-fission and symmetric fragmentation may occur.

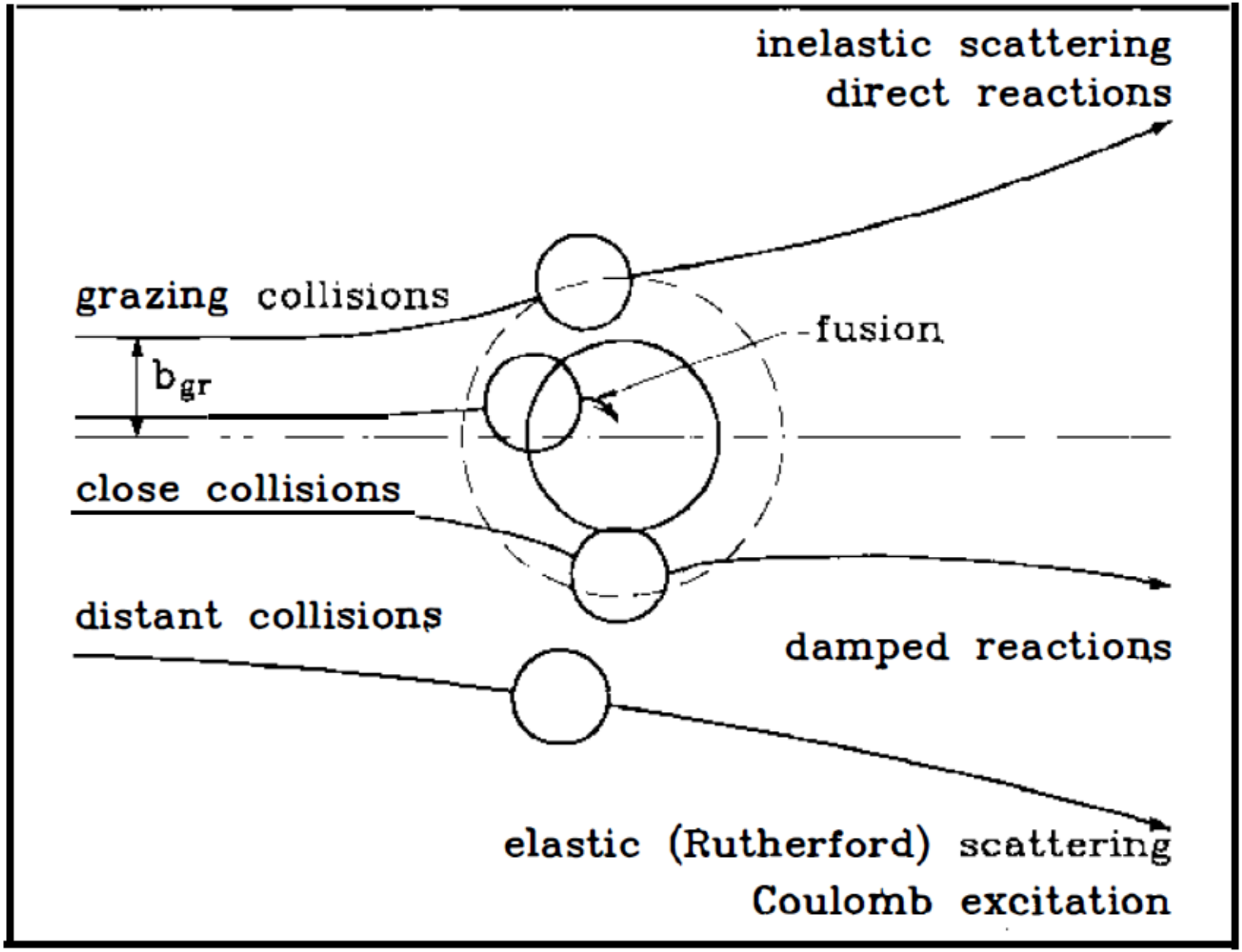

Figure 1 Classes of heavy-ion collisions associated with different values of impact parameters.

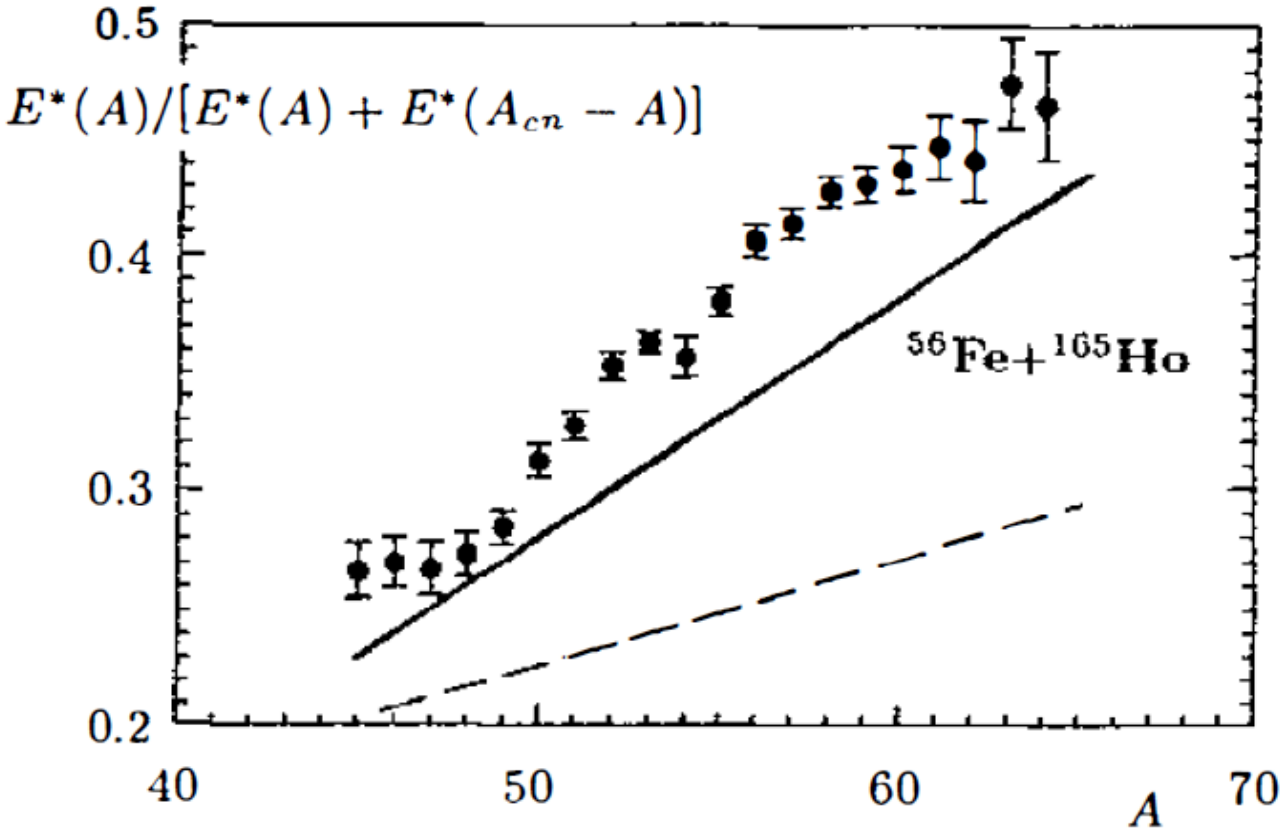

Figure 2 Fraction of the total excitation energy acquired by projectile-like fragments (PLFs) from the reaction $^{165}Ho + ^{56}Fe$ versus mass number A of the PLF, as predicted by the "random neck rupture model" (*solid curve*). The dashed curve reflects the equilibrium partition of the thermal energy, and the circles represent uncorrected data. $E^*(A)$ and $E^*(A_{cn} - A)$ denote the excitation energies of the PLF and the target-like fragment, respectively, and A_{cn} is the atomic number of the composite system (from 12).

J. Tõke and W.U. Schröder, Annu. Rev. Nucl. Part. Sci. 1992.42:401-446

Nonequilibrium Excitation-Energy Division in Deeply Inelastic Collisions

R. Vandenbosch, A. Lazzarini, D. Leach, D.-K. Lock, A. Ray, and A. Seamster
Nuclear Physics Laboratory, University of Washington, Seattle, Washington 98195

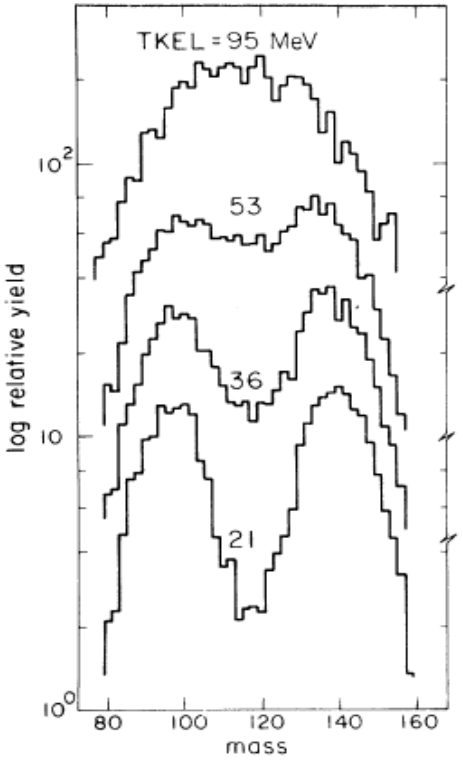

FIG. 1. Samples of fission-fragment mass distributions (lab system) at several different total kinetic energy losses (TKEL). The mean Z values of the fissioning nucleus, as inferred from the Z of the projectilelike fragment, increase from 92.8 to 93.3 with increasing energy loss.

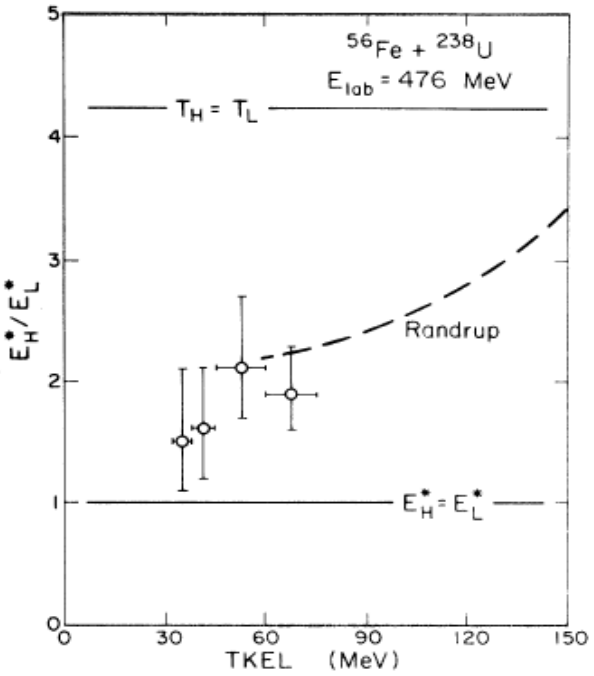

FIG. 2. Dependence of the ratio of the excitation energy of the heavy fragment to that of the light fragment as a function of the total excitation energy. The values expected in the limits of equal division of the excitation energy and of division according to the mass ratio (equal temperatures) are shown by horizontal lines. Also shown are the results of a transport-model calculation by Randrup.

The results obtained in this experiment demonstrate the possibility of the *"element“* approach in studying nuclear reactions with very heavy ions. Transfer reactions with 4°Ar have been shown to occur both in the form of quasielastic and deep inelastic processes.. Deep inelastic processes make a noticeable contribution to few-nucleon transfer reactions and are dominant in *multinucleon* reactions. *In* such processes all the kinetic energy of nuclear collisions is spent in the rearrangement and excitation of nuclei.. The transfer of a considerable number of nucleons from a heavy ion to the target nucleus with a noticeable cross section indicates the possibility of using such processes for the synthesis of transuranic elements and, possibly, of superheavy nuclei in a new region of stability. It is worth noting that the large width of the energy spectra of light products increases the probability of processes resulting in the weak excitation of the final heavy products.